Progress in Oceanography 219 (2023) 103150

Contents lists available at ScienceDirect

Progress in Oceanography

journal homepage: www.elsevier.com/locate/pocean

Lack of strong seasonality in macrobenthic communities from the northern Barents Sea shelf and Nansen Basin

Èric Jordà-Molina [a,*], Arunima Sen [b,a], Bodil A. Bluhm [c], Paul E. Renaud [d,b], Maria Włodarska-Kowalczuk [e], Joanna Legeżyńska [e], Barbara Oleszczuk [e], Henning Reiss [a]

[a] Nord University, Faculty of Biosciences and Aquaculture, 8049 Bodø, Norway
[b] University Centre in Svalbard (UNIS), Longyearbyen N-9170, Norway
[c] UiT – The Arctic University of Norway, N-9037 Tromsø, Norway
[d] Akvaplan-niva, Fram Centre for Climate and Environment, N-9296 Tromsø, Norway
[e] Institute of Oceanology Polish Academy of Sciences, Powstańców Warszawy 55, 81-712 Sopot, Poland

ARTICLE INFO

Keywords:
Benthic community dynamics
Phenology
Arctic
Functional traits
Taxonomic structure
Continental Shelf

ABSTRACT

The Barents Sea has been coined 'the Arctic hotspot' of climate change due to the rapidity with which environmental changes are taking place. This transitional domain from Atlantic to Arctic waters is home to highly productive benthic communities. This system strongly fluctuates on a seasonal basis in its sympagic-pelagic-benthic coupling interactions, with potential effects on benthic standing stocks and production. Recent discoveries have questioned the marked seasonality for several high Arctic seafloor communities in coastal waters of Svalbard. Still, the seasonal variability of benthic process in the extensive Barents Sea open shelf remains poorly understood. Therefore, we studied the seasonality of macrofauna communities along a transect in the northwestern Barents Sea comprising two hydrographic domains (Arctic vs. Atlantic Water, across the Polar Front) and three geomorphological settings (shelf, continental slope and abyssal plain). Overall, we did not find strong signs of seasonal variation in taxonomic community structure and functional diversity. However, we found some weak signs of seasonality when examining each station separately, especially at a station close to the Polar Front, with high seasonal fluctuations in abiotic drivers indicating a stronger pelagic-benthic coupling. The lack of seasonality found both at the shelf stations south and north of the Polar Front could be related to organic matter stored in the sediments, reflected in constant levels of total organic carbon in surface sediment across time for all stations. We did observe, as expected, highly spatially structured environmental regimes and macrofauna communities associated to them from shelf to slope and basin locations. Understanding the underlying spatio-temporal mechanisms by which soft-bottom benthic communities are structured along environmental gradients is necessary to predict future impacts of climate change in this area. Our results indicate that short-term climate driven changes in the phenology of pelagic ecosystem components might not be directly reflected in the Arctic benthic system, as seafloor processes seem to be partially decoupled from those in the overlying water.

1. Introduction

The Arctic marine ecosystem is a highly seasonal system (Walsh, 2008). Extreme light regime shifts occur on an annual basis from midnight sun periods with 24 h sunlight in summer to permanent dusk throughout the polar night in winter. This marked transition governs seasonal air temperatures which, in turn and together with ocean–atmosphere interaction processes, drives one of the most characteristic features of this region: the seasonal sea ice. Not only is the abiotic component of this system in constant transition, but also primary producers are phenologically tied to its seasonal fluctuations (Wassmann et al., 2011; Leu et al., 2015). Spring blooms of short lived pelagic and sympagic (ice associated) algae characterize the seasonality in Arctic primary production, which sustains the whole Arctic food-web, including seafloor communities (Sakshaug et al., 2009).

High seasonality characterizes processes occurring in the pelagic realm of marine Arctic environments. For instance, peak abundance and biomass of primary producers and zooplankton communities in the sea

* Corresponding author.
E-mail address: eric.jorda-molina@nord.no (È. Jordà-Molina).

https://doi.org/10.1016/j.pocean.2023.103150

Available online 12 October 2023

ice and the water column typically occur around early spring (Hassel, 1986; Wassmann et al., 1999; Weydmann et al., 2013), followed by a sharp decrease in winter, when a lot of zooplankton species enter diapause in deeper waters (Daase et al., 2013). In Arctic shelf seas, such as the Barents Sea, a strong sympagic-pelagic-benthic coupling has traditionally been posited to govern the tight connectivity between the sea ice, water column and seafloor associated communities (Grebmeier et al., 1988; Wassmann et al., 1991; Graf, 1992; Søreide et al., 2013) through the cascading transfer of organic matter (OM) (i.e. vertical flux of particles) (Renaud et al., 2008; Wassmann et al., 2008; Wassmann and Reigstad, 2011). Thus, although expected, seasonal dynamics of macrobenthic communities and seafloor processes in the Arctic have received very little attention, outside of some intertidal (Pawłowska et al., 2011; Naumov, 2013) coastal/fjord studies Kędra et al., 2012; Włodarska-Kowalczuk et al., 2016; Morata et al., 2020) around Svalbard waters. Until recently it was thought that benthic communities entered a state of dormancy during the polar night, when little photosynthetic activity is possible and very little OM is exported to depths (Renaud et al., 2020). Recent studies, however, have demonstrated that benthic organisms do grow and reproduce during this time of the year, most likely relying on stored energy reserves or on detrital and advected resources (Berge et al., 2015).

Renaud et al. (2008) suggested that responses to seasonal food pulses are reflected at variable temporal scales in seafloor communities depending on the process in question. For instance, feeding rates of benthic organisms and sediment oxygen demand (SOD) rates respond within a few hours to weeks to short-term pulses of organic carbon reaching the seafloor. In contrast, responses of biomass and other benthic community metrics fluctuate on longer time-scales of weeks to months in response to seasonal fluctuations in OM input (Carroll et al., 2008; Renaud et al., 2008). However, food supply is not the only factor that can influence seasonality in benthic community processes. Species-specific reproduction strategies, recruitment and settlement of meroplankton larvae, together with post-settlement processes and species interactions, are also factors that can determine the seasonal dynamics of benthic adult populations (Thorson, 1950). Here, benthic functional community composition and its phenological dynamics might provide further insights into the responses of benthic communities to seasonal fluctuations in primary production and abiotic environmental changes.

Soft-bottom benthic communities (mainly dominated by macrofauna representatives) have key roles in biogeochemical processes (Klages et al., 2004; Bourgeois et al., 2017; Snelgrove et al., 2018; Solan et al., 2020) as they are responsible for remineralizing the OM that reaches the seafloor, closing the carbon cycle and replenishing nutrients to the water column which fuel pelagic primary production (Thamdrup and Canfield, 2000). Many macrofaunal traits (i.e., morphological, behavioral and life history traits) can give insights about the ecological roles displayed by these communities (Oug et al., 2012; Degen et al., 2018). For instance, their feeding habits can reflect hydrodynamic conditions and carbon availability at the seafloor (Sutton et al., 2021).

Recent studies have hypothesized that increased effects from climate change, such as ocean warming, sea ice cover retreat and increased primary production and input of OM to the seafloor will cease the seasonality of benthic processes and activities (Morata et al., 2020). This reduction in seasonality might increase the benthos' resilience to intra-annual variability in pelagic primary production, which is expected to shift its phenological timing in high Arctic regions. However, in the long run, it could reduce the communities' functional diversity and redundancy by favoring deposit-feeding taxa over suspension feeders, leading to a decoupling from pelagic-benthic interactions and increasing detrital energy pathways, with unknown tipping points and consequences to the ecosystems' stability (Morata et al., 2020). Therefore, understanding spatio-temporal dynamics of macrobenthic taxonomic and functional community composition is critical to anticipate shifts in seafloor biogeochemical processes that could alter the whole ecosystem function (Degen et al., 2018). Spatio-temporal relationships between macrobenthic taxonomic diversity and functional diversity have yielded diverging results in the Arctic in that some showed a strong link of taxonomic and functional patterns (Kokarev et al., 2017; Włodarska-Kowalczuk et al., 2019) and others a weak link (Cochrane et al., 2012). However, no studies to our knowledge have attempted to assess the dynamics of functional diversity on a seasonal basis and whether it fluctuates in a concomitant temporal scale or not with the community taxonomic structure.

Given the knowledge gaps in seasonality of high Arctic macrobenthic community composition and functional diversity, we conduct here the first seasonal study of macrobenthos in the open northern Barents Sea. We sample a transect with variable influence of sea ice and water masses to gain insight into potential trajectories in system change due to regional warming trends: from the Atlantic-influenced southern, and Arctic-influenced northern Barents Sea, to the continental slope and the adjacent Nansen Basin. The main aims of the study are (i) to assess the seasonality of macrobenthic community composition and functional diversity and (ii) to identify if the temporal dynamics of environmental variables are responsible for the structure of communities in these very distinct hydrographical and ecological settings. We hypothesize that seasonality in environmental variables such as sea ice cover, water mass properties and in OM export to the seafloor will be main drivers of spatio-temporal changes in the taxonomic and functional structure of benthic communities. We hypothesize that macrofauna abundances (and to a lower extent biomass) may reflect to some extent seasonal patterns of productivity in the overlying waters, increasing during the spring bloom, and decreasing during the polar night. Finally, we expect to find different timing in macrofauna seasonality along the transect following the space–time substitution paradigm, which states that bloom phenology is delayed at higher latitudes due to more persistent sea-ice cover (Wassmann et al., 2020), making seasonal patterns along this region site-specific and context dependent.

2. Material and methods

2.1. Study area

The Barents Sea comprises a transitional domain between warm, Atlantic water masses in the south and cold, Arctic water masses in the north, separated by the Polar Front, an oceanographic feature characterized by high biological productivity (Sakshaug et al., 2009). The Barents Sea shelf, with depths ranging from ca. 100 to 300 m, is bathymetrically complex, with several troughs and banks having different granulometric properties, presenting higher clay and silt fractions in the troughs and sandier sediments in the shallower areas (Carroll et al., 2008). To the north, the shelf break leads to a steep continental slope, with a dynamic and small-scale heterogenous geomorphological setting comprising a variety of troughs, furrows, channels, canyons and mouth fans ending with a rugged topography further downslope (Kollsgård et al., 2021). The adjacent Nansen Basin presents an abrupt transition towards the oceanic environment with fine silt and clay types constituting an average of above 90 % of the total sediment (Husum et al., 2015). The West Spitsbergen Current (WSC) flows along the Norwegian shelf break northwards towards the Fram Strait, bringing warm Atlantic Water to the north. Once it crosses the Yermack Plateau, it evolves as the Svalbard Branch, which flows along the continental slope north of Svalbard and occasionally protrudes into the northern Barents Sea shelf (Fig. 1).

The study area comprised a transect of seven stations in the northwestern Barents Sea, east of the Svalbard Archipelago ranging from 76.0°N to 81.9°N. Four of these stations were located on the shelf: P1 south of the Polar Front, and P2, P4 and P5 north of it. Station P6 was located on the continental slope, station P7 in the southern Nansen Basin, and station SICE4 in the deep Nansen Basin (Fig. 1 **and** Table 1).

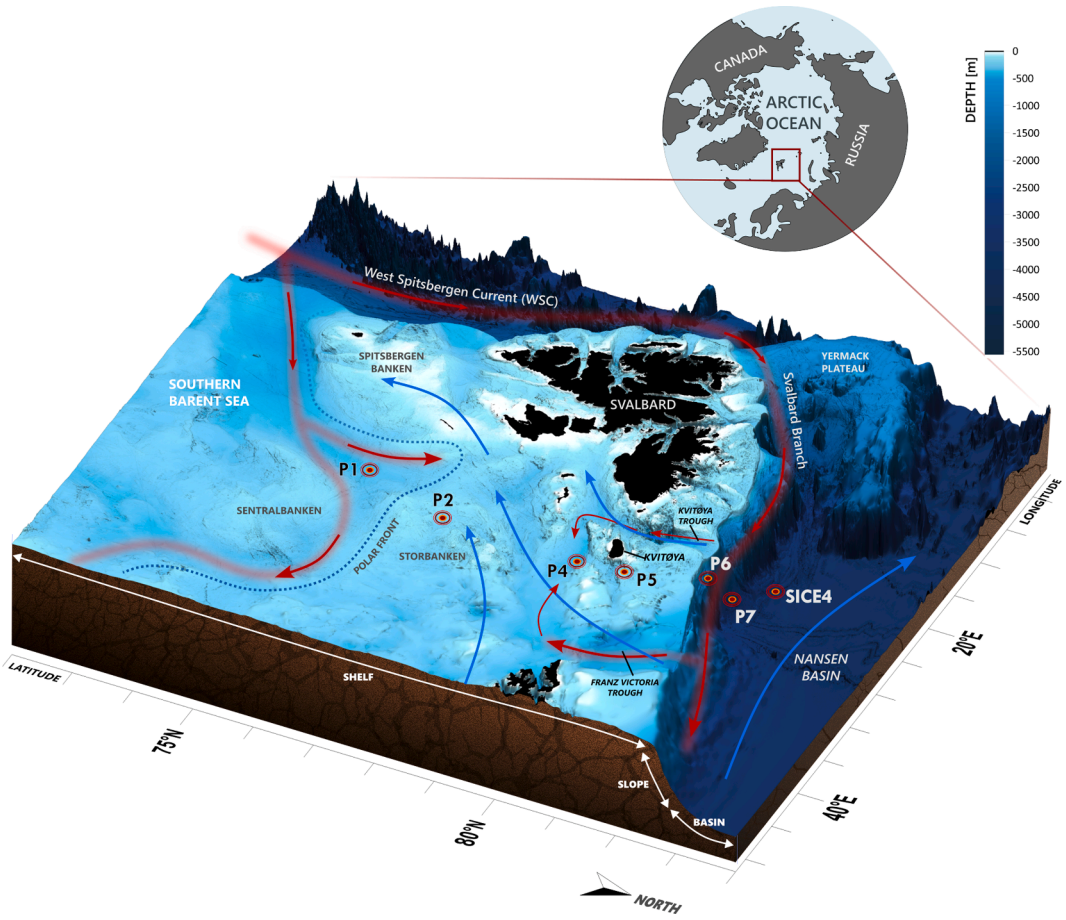

Fig. 1. Map of the northwestern Barents Sea with the location of the sampling stations along the sampling transect (from P1 to SICE4) indicated with red dots. Cold Arctic currents are indicated with blue arrows and warm Atlantic currents are indicated with red arrows. The stippled line indicates the approximate position of the Polar Front. Bathymetric data source. GEBCO Compliation Group, 2022.

2.2. Sampling and sample processing

Sampling was conducted on board of the Norwegian icebreaker R/V *Kronprins Haakon* in August 2019, December 2019, March 2021 and May 2021 (Table 1). Due to the COVID-19 pandemic, the sampling planned for March and May 2020 was deferred to 2021. Therefore, a gap-year exists between the samples from December 2019 and March 2021 in which samples were not available to assess a consecutive annual cycle.

At each station and season, three box core replicates (0.25 m^2) were retrieved (Table 1). Stations P5 and SICE4 were only sampled in August 2019, yet were included in this paper to give a better resolution for the spatial context of the transect. However, since seasonality was the main focus of our study, they were not included in most of the analyses focusing on seasonal variations.

2.2.1. Water masses and sea ice concentration

At each station bottom water temperature and bottom salinity were measured with the ships' conductivity, temperature, depth (CTD) recorder. Following the TEOS-10 convention (IOC, SCOR and IAPSO, 2010) and using the R package "gsw", practical salinity unit (PSU) values were converted to absolute salinity and in-situ temperature values were first calculated to potential temperature prior to obtaining conservative temperature values. Using the same package, potential density was calculated from absolute salinity and in-situ temperature values with sea level pressure as reference. From this, bottom water masses were assigned to each station and for each time of the year (Fig. 2) following the water mass definitions from the Nansen Legacy (Sundfjord et al., 2020).

Daily sea ice concentrations at each station location were retrieved as a 6.25 km gridded product of sea ice concentration from a repository of the University of Bremen based on AMSR-E and AMSR2 passive microwave sensors (https://seaice.uni-bremen.de/sea-ice-concentration/amsre-amsr2/information/) for the years 2019, 2020 and 2021. Sea ice concentration values were extracted for each date of the station/season events (see Table 1 for dates) following the python code from Steer (2022) to use as environmental predictor. Since sea ice concentration was the only environmental parameter for which continuous records were available during the gap year in 2020, we used this environmental data to asses qualitatively if the surface water conditions remained relatively constant or not between the sampled years 2019 and 2021.

2.2.2. Granulometry, total organic carbon (TOC) and sediment pigments

A 5.5 cm in diameter plastic sub-core from each box core replicate (three replicates in total) as described in Ricardo de Freitas et al. (2023, under review this issue) and the core was sliced every centimeter from the surface. Sediment granulometry characteristics (mean grain size, silt content, clay content and sand content) for the 0–2 cm surface sediment layer (average between the 0–1 and 1–2 slices) and total organic carbon content (TOC%) for the 0–1 cm surface sediment layer were determined as described in Ricardo de Freitas et al. (2022a, 2022b, 2022c, 2022d) and Ricardo de Freitas, et al. (2023, under review) and resulting data used as published in Ricardo de Freitas et al. (2022a, 2022b, 2022c, 2022d) and Ricardo de Freitas et al. (2023, under review this issue).

In order to characterize sediment pigments of the surface seafloor (chlorophyll *a* and phaeopigments) one replicate core of 4.7 cm in diameter was retrieved from each of the three box cores replicates. Cores

Table 1
Overview of the sampling conducted in the present study. For each station and season (month) of the year, three box core replicates were deployed (BC-1,2&3). For each box core replicate, the exact coordinates in decimal degrees (°)) and depths (m) are given. At each station/season, five cylindrical core replicates of 11.7 cm diameter (ø) were randomly subsampled from each of the three box core replicates, trying to maximize subsampling from each box core as much as possible. These five core replicates are considered as the macrofauna replicates used for the analyses in this study. For each station/season, the dates in which the three box core replicates were deployed are given. Note that at stations P6 and P7 coordinates and depths differed more than at shelf stations between box core replicates and seasons due to difficulties to maintain the ship's position against strong drifting sea ice conditions.

Station	Month and Year (date of deployment)	Box Core replicate	Number of core Replicates (ø 11.7 cm)	Coordinates (°N,°E)	Depth (m)
P1	August	BC-1	2	75.99, 31.22	326.1
(Atlantic Station)	*(09.08.2019)*	BC-2	2	75.99, 31.22	326.0
		BC-3	1	75.99, 31.22	325.0
	March	BC-1	2	76.00, 31.21	324.9
	(06.03.2021)	BC-2	2	76.00, 31.21	324.8
		BC-3	1	76.00, 31.22	325.2
	May	BC-1	2	76.00, 31.22	325.6
	(01.05.2021)	BC-2	1	76.00, 31.22	326.1
		BC-3	2	76.00, 31.22	326.1
P2	August	BC-1	2	77.50, 34.00	188.5
(Polar Front Station)	*(12.08.2019)*	BC-2	1	77.50, 34.00	188.5
		BC-3	2	77.50, 34.00	188.8
	March	BC-1	3	77.51, 33.70	167.8
	(07.03.2021)	BC-2	1	77.52, 33.65	162.6
		BC-3	1	77.53, 33.60	169.8
	May	BC-1	3	77.50, 34.00	190.3
	(02.05.2021)	BC-2	2	77.50, 34.00	190.8
		BC-3	-	77.50, 34.00	190.8
P4	August	BC-1	2	79.75, 34.02	333.8
(Arctic Station)	*(14.08.2019)*	BC-2	1	79.74, 34.00	332.7
		BC-3	2	79.75, 34.03	331.1
	December	BC-1	2	79.76, 34.00	330.0
	(09.12.2019)	BC-2	1	79.75, 34.00	337.0
		BC-3	2	79.74, 34.00	338.0
	March	BC-1	1	79.77, 33.61	326.9
	(11.03.2021)	BC-2	3	79.77, 33.59	320.5
		BC-3	1	79.76, 33.52	331.9
	May	BC-1	2	79.75, 34.00	335.3
	(06.05.2021)	BC-2	1	79.76, 33.99	330.1
		BC-3	2	79.76, 34.00	326.8
P5	August	BC-1	5	80.50, 34.02	160.7
(Arctic Station shallow)	*(16.08.2019)*				
P6	August	BC-1	2	81.55, 30.85	856.6
(Continental Slope Station)	*(19.08.2019)*	BC-2	-	81.53, 30.96	806.3
		BC-3	3	81.54, 30.88	829.1
	December	BC-1	2	81.54, 30.94	848.0
	(05.12.2019)	BC-2	1	81.55, 30.86	879.0
		BC-3	2	81.55, 30.89	870.0
	March	BC-1	1	81.55, 30.85	869.1
	(15.03.2021)	BC-2	3	81.55, 30.85	872.3
		BC-3	1	81.55, 30.86	868.3
	May	BC-1	2	81.54, 30.87	824.2
	(11.05.2021)	BC-2	1	81.56, 30.85	953.8
		BC-3	2	81.56, 30.85	916.7
P7	August	BC-1	3	81.73, 28,67	2648.9
(Nansen Basin)	*(22.08.2019)*	BC-2	2	81.67, 28.79	2349.3
		BC-3	-	81.67, 28.81	2329.0
	March	BC-1	3	81.73, 28.67	2671.1
	(18.03.2021)	BC-2	2	81.73, 28.67	2668.0
	May	BC-1	2	81.84, 30.76	3102.6
	(15.05.2021)	BC-2	1	81.81, 30.85	3083.5
		BC-3	2	81.79, 30.95	3065.6
SICE4	August	BC-1	1	81.99, 24.53	3603.8
(Nansen Basin)	*(23.08.2019)*	BC-2	2	81.99, 24.74	3603.8
		BC-3	2	81.99, 24.80	3604.0

were sliced into sections of 0–1 cm and 1–2 cm and stored in whirl-pack bags wrapped in aluminum foil at −20 °C. Pigments were analyzed according to Holm-Hansen et al. (1965). Briefly, sediment samples were thawed in the dark at 4C and pigments were extracted in 100 % acetone in the freezer for 24 h. Samples were centrifuged (6000 rpm for 15 min) and aliquots of the supernatant were measured on a Turner model 10-AU fluorometer before and after acidification with 1 N HCl. Data were standardized to mass per m^2. The sediment pigment data was used as published in Akvaplan-niva (2023a, 2023b, 2023c, 2023d). The two slices (0–1 and 1–2 cm) were then summed together to represent the sediment pigment concentrations of the 0–2 cm surface sediment layer.

2.2.3. *Macrofauna community*

After carefully removing the overlying water from the sediment surface, 11.7 cm diameter plastic cylindrical cores were pushed into the sediment of the box cores. In total, five replicate cores (taken randomly throughout the three box core replicates) were sampled at each station and season for macrofauna community analysis. Samples were sieved over a mesh size of 0.5 mm and preserved in 4 % formaldehyde solution buffered with borax. In the laboratory, organisms were identified to the

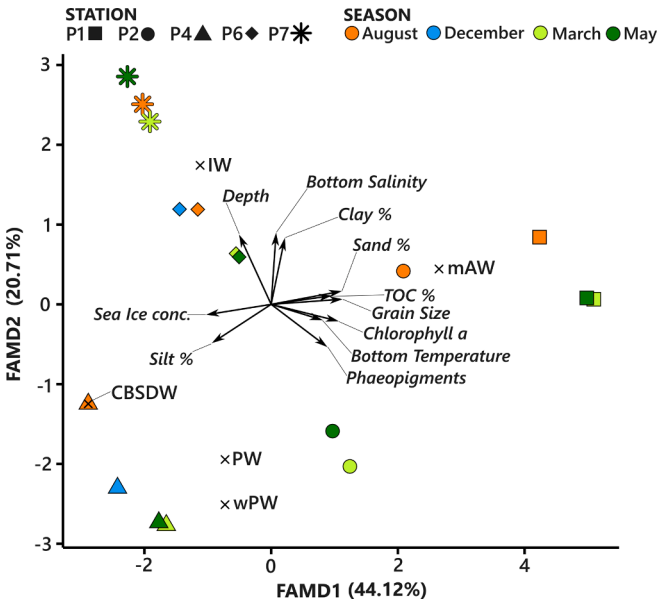

Fig. 2. Factor analysis of mixed data (FAMD) of quantitative (black arrows) and qualitative (water masses as black crosses) environmental variables and sampling stations in the northern Barents Sea across four seasons. The inertia explained by each axis is expressed in percentage. Bottom water-masses are derived from bottom water temperatures and salinities. mAW = modified Atlantic Water; PW = Polar Water; wPW = warm Polar Water; CBSDW = Cold Barents Sea Dense Water; IW = Intermediate Water and PW = Polar Water; based on definitions from Sundfjord et al. (2020).

lowest taxonomic level possible (depending on preservation state of specimens or taxonomic literature available) and counted at the Institute of Oceanology of the Polish Academy of Sciences (IOPAN) labs. Also, the weight (g) of the identified taxa was assessed as wet weight for the lowest taxonomic level possible matching the taxonomic identification. Accepted scientific names were retrieved from the World Register of Marine Species (WoRMS) (December 2021).

2.3. Data analysis

2.3.1. Environmental drivers

In order to explore the seasonality and spatial structure in environmental variables, a factor analysis of mixed data (FAMD) was performed to visualize differences in bottom water-mass properties, sediment parameters and sea ice cover across stations and seasons using the *FAMD* function from the R package "FactoMineR" (Lê et al., 2008). FAMD is a principal component method, similar to Principal Component Analysis, that allows for including both quantitative and qualitative data (Pagès, 2004). Sediment parameters such as grain size and proportions of silt, clay and sand were only available for August 2019 but were assumed to remain constant across seasons given the short amount of time between sampling events.

2.3.2. Macrofauna taxonomic composition and diversity

Univariate alpha diversity indices (species richness (S), Shannon diversity index (H' (log e)) and Pielou's evenness (J')) were calculated for each replicate with the R package "vegan" (Oksanen et al., 2013). In order to test for significant differences of alpha diversity indices across seasons for each station, a Kruskal-Wallis test was performed using the R package "stats" (R Core Team, 2022). After that, a rank sums Conover-Iman test of multiple comparisons with Bonferroni p-adjusted values was performed with the R package "conover.test" (Dinno and Dinno, 2017) to identify which pairs of seasons were significantly different.

A non-Metric Multidimensional Scaling Analysis (nMDS) was performed with both the Hellinger transformed abundance of macrofauna (which allows to work in the Euclidean space) and the square-root transformed biomass for each station and season using the *metaMDS* function from the R package "vegan". For the Hellinger-transformed abundance-based ordination, Euclidean dissimilarity distances were applied, while for the biomass-based ordination, Bray-Curtis dissimilarity distances were used. Environmental variables were fitted onto the ordination as vectors of correlation with the *envfit* function. A UPGMA cluster analysis of the Hellinger transformed abundance was performed using the *hclust* function from the R package "stats" to validate the grouping patterns from the nMDS. Additionally, a heatmap was used to visualize the most abundant species (individuals with more than 10 individuals for the sum of all samples in the study) below the cluster dendrogram with the R package "pheatmap" (Kolde, 2019). A two-way PERMANOVA analysis was performed with the function *adonis2* from the R package "vegan" to test for significant differences in the multivariate macrofauna community for Hellinger transformed abundances across the different stations and seasons. At the same time, PERMANOVA analysis with 9999 permutations was performed for each station separately to test for significant differences across seasons. Post-hoc pair-wise tests were conducted to search for significantly different pairs, using the Bonferroni method to correct the p-values for multiple testing with the *pairwise.adonis2* function from the R package "pairwiseAdonis" (Martinez Arbizu, 2017). To validate that the differences detected were not affected by heterogeneity of variances across seasons, a test of multivariate homogeneity of groups dispersions was conducted for the Euclidean distance-matrix of Hellinger transformed macrofauna abundance and traits (CWM) for each individual station across the factor seasons with the function *betadisper* from the R package "vegan". This is a multivariate analogue of Levene's test for homogeneity of variances in which the distances of each observation to the group centroid (in this case the factor "seasons") are tested to check whether one group is significantly more variable than the other. The test of significance was performed using the *permutest.betadisper* function from the R package "vegan" with 9999 permutations.

To identify which samples from which seasons were driving the most important betadiversity differences seasonally, local contributions to beta diversity (LCBD) values were calculated with the function *beta.div* of "adespatial" package (Dray et al., 2018) using Hellinger dissimilarity coefficients (Legendre and Borcard, 2018; Legendre and De Cáceres, 2013). LCBD indices represent the degree of uniqueness of the samples in terms of community composition (Legendre and De Cáceres, 2013) and show how much each observation contributes to beta diversity; a sample unit with an LCBD value of 0 would have the species composition of the average centroid for all sites. LCBD values can be tested for statistical significance by random, independent permutations of the species matrix. Adjusted p-values (Holm correction method for multiple testing) for the LCBD values were calculated with 999 permutations, testing the null hypothesis (*Ho*) that species are randomly distributed and independent of one another across seasons (Legendre and De Cáceres, 2013). LCBD values were calculated for each station separately across sampled seasons in order to identify seasons that were significantly unique in taxonomic composition compared to the average community composition of all the seasons.

2.3.3. Biological traits approach (BTA) and functional diversity

For the functional traits analysis, biological traits were retrieved from the Arctic Traits Database (Degen and Faulwetter, 2019). Seven fuzzy coded functional traits were used (size, body form, living habit, adult movement, larval development, feeding habit and environmental position) with a total of 32 categories (**Table S1** in Supplementary material). For each taxon, trait categories were given a value from zero to three, with zero meaning no affinity for that category and three meaning exclusive affinity for that category. For unavailable traits for some of the taxa at the species level, traits were retrieved for the genus or family level. In order to calculate functional diversity indices, fuzzy coded traits were standardized in proportions from 0 to 1 using the

function *prep.fuzzy.var* from the R package "ade4" (Dray and Dufour, 2007) and a matrix distance was calculated with the *dist.ktab* function. Using the function *dbFD* from the R package "FD" (Laliberté et al., 2014), functional richness (FRic), functional evenness (FEve), functional dispersion (FDis) and functional redundancy (Fred = FDis/H') were calculated. FRic indicates the amount of functional space occupied by all species in the community and does not take into account the abundance of organisms; FEve accounts for the evenness in the distribution of the abundance of organisms in the functional space; FDis is the mean distance in the trait space of each species to the centroid of all species in the community, which can be weighted by the abundances, shifting the centroid towards the more dominant taxa (Ahmed et al., 2019; Carmona et al., 2016). Functional redundancy (Fred, calculated as the ratio of FDis/H'), indicates to what degree different taxa occupy the same functional space (i.e. display the same traits). Whenever this ratio decreases, functional redundancy increases (van der Linden et al., 2012). Functional diversity indices were tested for significant differences across seasons at each station with a Kruskal-Wallis test followed by a Conover-Iman test of multiple comparisons with Bonferroni p-adjusted values the same way as was done for the alpha-diversity indices.

The community weighted mean (CWM) of functional traits weighted by the Hellinger-transformed abundances was calculated using the function *functcomp* from the package "FD", generating a Stations/Seasons × Traits matrix, where trait categories are expressed in proportions adding up to 1 based on the weight of Hellinger transformed abundance. A Fuzzy Correspondence Analysis (FCA) (Chevene et al., 1994) was performed with the CWM matrix to visualize the contribution of traits and their modalities in differentiating the functional structure among stations and seasons. This was done with the *dudi.fpca* function from the R package "ade4".

For the CWM weighted abundance trait matrix, a two-way PERMANOVA analysis was performed to test for significant differences in trait composition for the different stations and seasons, the same way as for the taxonomic community composition. At the same time, PERMANOVA analysis with 9999 permutations was performed for each station separately to test for significant differences across seasons. Post-hoc par-wise tests were conducted to search for significantly different pairs, using the Bonferroni method to correct the p-values for multiple testing, the same way as for the taxonomic community composition. Also, multivariate heterogeneity of variances were tested the same way as for the abundance dataset (see above).

2.3.4. Variation partition of macrofaunal community with environmental variables

Redundancy analysis (RDA) was used to partition the variation within the Hellinger-transformed abundance and the macrofauna functional composition (CWM Hellinger transformed) datasets on the set of environmental predictor variables, the spatial structure of the sampling stations (spatial-autocorrelation) using Moran Eigenvector Maps (MEMs) and the temporal structure (seasonality, but also other time scale fluctuations) using Asymmetric Eigenvector Maps (AEMs) based on the sampling seasons. MEMs are orthogonal vectors calculated through decomposition of the Moran's I coefficient to maximize spatial autocorrelation. These spatial predictors can then be used in variation partition analysis to explicitly account for spatial structure (Dray et al., 2012). MEMs were calculated based on the geographical coordinates of sampling locations (original targeted coordinates for each station were used instead of the exact coordinates of sampling events, since they generally did not vary significantly between replicates and seasons) (excluding P5 and SICE 4) using the *list.explore()* function from the R package "adespatial". For that we input the coordinates, used "distance" graph type, and after the Euclidean distances between sites were calculated, we defined the weights of the spatial weighting matrix as *1-d/*max*(d)* and finally we obtained the MEMs (the number of which is n-1, where n is the number of sites) by using the standardization style "B", which is the basic binary coding. For all these intermediary steps we used the R packages "sp" and "spdep" (Pebesma and Bivand, 2005; Bivand et al., 2008) (to see the different calculated MEMs the reader is referred to **Fig.S5** from the Supplementary Material). AEM is an eigenfunction method suitable to model multivariate directional processes like temporal change of species abundance data. By incorporating AEMs as constraining temporal predictors one can account for temporal autocorrelation (or temporal structure) in the abiotic drivers or in the species matrix itself (Legendre and Gauthier, 2014). To account for the irregular intervals between sampling events, dummy sampling events were added on the 15th day of every month when no samples were collected, starting the 15th of August and finishing the 15th of May. Based on results from the macrofauna community taxonomic and functional structure (see Results section), which did not show extreme differences between the seasons from 2019 and 2021, we considered seasons as being from consecutive years, instead of taking into account the gap year between 2019 and 2021 (see Discussion section). AEMs were then calculated using the time between neighboring dates as edge weight with the function *aem.time* from R package "adespatial". In principle, AEMs as temporal predictors are essentially n-1 sine waves of decreasing wavelength, where n is the total number of sampling dates; here n = 10, including the dummy variables). The smallest AEM, AEM_1 depicts long time scale fluctuations and the biggest AEM, AEM_{10} depicts smaller time-scale variations (**Fig. S6**).

The environmental variables used as community predictors in the RDA analysis were previously standardized. From the granulometric parameters, only the mean grain size was used as surrogate for the silt, clay and sand content variables to avoid high collinearity between environmental predictors (**Fig. S1**). For the sediment pigments and TOC (%) values, the mean between the three replicate samples (or less replicates when not available) from the box core replicates at each station/season event were used as predictor variables (see **Table S2**). For the response variables, the Hellinger transformed macrofauna abundance and functional composition based on Hellinger transformed abundance CWM, the five core replicates (see Table 1) were considered separately.

Prior to variation partitioning, the three sets of environmental, spatial auto-correlation predictors (MEMs) and temporal predictors (AEMs) were individually subjected to forward selection (FWS) for both the abundance and traits (CWM) datasets using a double-stopping criterion (Blanchet et al., 2008) to avoid overestimation of the explained variation. In this approach, variables are added to the model in order of decreasing explanatory power until no variable adds significantly to the explanatory power or until the R^2-adjusted exceeds the R^2-adjusted of the full model (Blanchet et al., 2008). The variation partition analysis was performed with the *varpart* function of the R package "vegan".

Another set of variation partition analyses were performed for each station individually in order to assess the contributions of seasonality (this time without spatial predictors (MEMs)) for both the abundance and traits (CWM) datasets. In this case, depth and sediment grain size parameters were excluded, as they were not expected to vary across seasons. Both AEMs and environmental variables were subjected to forward selection prior to variation partitioning with the same procedure as in the first variation partition sets for the whole transect.

3. Results

3.1. Seasonality and spatial structure in environmental variables

The FAMD analysis revealed clear environmental differences among stations (Fig. 2). For the first axis, which explained most of the variation (44.12 %), the southern stations P1 and P2 correlated positively with bottom water temperature, TOC, grain size, sediment phaeopigments and chlorophyll *a*; while stations from P4 northwards were characterized by higher sea ice concentration and silt fraction. At stations P1, and P4 and P6, but especially at station P4 the August conditions differed from December, March and May conditions along the second axis (which explained 20.71 % of the variation), which was mainly driven by the

small variations in bottom water salinity and the different water masses.

Station P2 had the highest seasonality in ice cover, with high cover in March and May, but open water conditions in August. Sea ice concentration at stations P4, P6 and P7 was higher than 80 % for all season, with very small variations in time. Station P1 was free of sea ice during all sampling seasons (Fig. 3, **Table S2**). The qualitative analysis of sea ice concentration during the gap year revealed that the year 2019 had generally higher sea ice cover than the end of 2020 and beginning of 2021, especially on the northern stations P6 and P7.

Bottom water temperatures at stations P1 and P6 were above or close to 0 °C for most of the seasons, while P7 had negative temperatures in all seasons. Stations P2 and P4 had the highest seasonal temperature variations, with values ranging from negative values in December and August to above 0 °C in spring (Fig. 3, **Table S2**). Bottom water salinity was nearly constant at all stations, between ca. 34.7 to 34.9 PSU (**Table S2**). Total organic carbon content in surface sediments (TOC) was highest at station P1 (1.9–2.1 %) compared to all the other stations north of the Polar Front (1.3–1.5 %) (Fig. 3, **Table S2**). No strong seasonal variations were observed at any of the stations (Fig. 3, **Table S2**). Chlorophyll *a* in sediments was mostly constant through seasons at stations P4, P6 and P7 (ranging between 2 and 4.1 mg/m^2 across those stations) (Fig. 3, **Table S2**). Much higher values were observed at stations P1 (12–9.5 mg/m^2) and P2 (11.5–5.9 mg/m^2), with the highest variations at the latter one, where the highest values were noted in August and the lowest in March (Fig. 3, **Table S2**). Sediment phaeopigments had lower values at stations P4, P6 and P7 (14.7–31.2 mg/m^2) compared to stations P1 (29.5–42.4 mg/m^2) and P2 (34.2–43.8 mg/m^2). Seasonal variations were observed in most stations, with lower values in August (and in December at P4 and P6) and highest in March/May (Fig. 3, **Table S2**). This was also reflected in the sediment pigment quality ratios (Chlorophyll *a*/Phaeopigments) indicating an overall lower food quality in March/May than in August/December (Fig. 3).

3.2. Seasonal and spatial patterns in macrofauna taxonomic structure

A total of 272 different taxa belonging to 8 phyla were identified, with Annelida and Mollusca being the most abundant, followed by Arthropoda and Echinodermata. Polychaeta was the most abundant class, contributing to 59 % of the total abundance, followed by Bivalvia (23 %), Malacostraca (7 %) and Ophiuroidea (3 %). Overall, polychaetes (phylum Annelida) dominated numerically at most stations, except at stations P2 and P5, where molluscs were almost equally abundant (Fig. 4**A**). No seasonal differences were found in total abundance at any station except for station P6, where abundance was significantly higher in December than in March and May (Fig. 4**B**). The total abundance at P2 and P5 was higher than for the other shelf stations, and the lowest abundance values were noted in the Nansen Basin (Fig. 4**B**). The only significant seasonal changes in biomass were observed for stations P2 and P6, with a significant increase in biomass from March to May at P2, and significantly higher biomass in August than in May at P6. As with abundance, total macrofauna biomass (Fig. 4**C**) was higher at shelf than slope and basin stations. In general, H' index was higher for shelf and slope stations than for the basin stations (Fig. 4**D**). Significant seasonal differences were only found at P1 (higher values in August compared to March) and P2 (higher values in March than in August and May). Taxon richness followed a similar pattern as abundances across stations, and seasonal significant differences were only found at station P2, with higher values in March compared to August (Fig. 4**E**). J' index values increased gradually with latitude, and seasonal changes were only found at station P2, with significantly higher values in March compared to August and May (Fig. 3**F**).

The cluster analysis revealed relatively stronger seasonal dissimilarities at stations P2, P4 and P6, while almost no dissimilarities were found at the Atlantic station P1 (Fig. 5). In addition, it revealed that the community at station P1 was more similar to P4 than to the neighboring station P2, due to the numerical dominance of the tube-building polychaete *Spiochaetopterus typicus* and high abundances of three other polychaete species: *Heteromastus filiformis*, *Spiophanes kroyeri* and *Anobothrus laubieri*. The two shallowest stations, P2 and P5, clustered together, both being dominated by bivalves such as *Macoma* sp., *Yoldiella solidula* and *Yoldiella lenticula*. At P2 polychaetes *Lumbrineris* sp., *Myriochele heeri* and *Galathowenia oculata* were also relatively numerous. Fauna at station P6 was clearly dominated by the polychaete *Prionospio cirrifera,* while station P7 had relatively high abundance of *Myriochele heeri* and *Siboglinum norvegicum* (Fig. 5 **and Table S3**).

The nMDS based on Hellinger transformed macrofauna abundance revealed a clear separation between the shelf stations (P1, P2, and P4) and the slope and basin stations (P6 and P7). Shelf stations also differed from each other in community composition, with P1 and P4 being more similar to each other than to P2. No clear seasonal differences were observed, as samples taken at different seasons tended to not form distinctive groups for a given sampling station (Fig. 6**A**). A similar pattern was observed for the macrofauna biomass, and in this case stations P1 and P4 stations were grouped even closer (Fig. 6**B**). Environmental variables that correlated best with the community composition of the deeper stations P6 and P7 were sea ice concentration, clay and silt fractions and bottom water salinity. In contrast, the shelf stations were positively correlated with sand fraction and mean grain size, sediment pigments, TOC and bottom water temperature.

LCBD map (Fig. 7) showed that March samples from P2 station had significantly higher LCBD values, indicating that those samples were more unique in community composition than the mean composition of the other seasons. At station P6, significantly higher LCBD values were found for May samples. Although not significant, station P4 had higher LCBD values in March too, while station P7 and P6 had higher values in May. Stations P1 had similar LCBD values for all seasons.

The PERMANOVA analysis based on abundance of macrofaunal community composition (Table 2) revealed significant differences across stations, seasons and the interaction of both. However, the R^2 explained by season (0.05) and the interaction of season and station (0.13) was much lower than for the factor station (0.39), indicating low contribution of the seasonality factor to the variation explained. At P1 significant differences in community composition were found only between August-May and March-May. For P2, P4 and P7 stations, significant differences were found between all pairs of seasons. For station P6, significant seasonal differences were found between all pairs of seasons except between August and December. Both stations P2 and P7 had highest R^2 values for the factor season (0.42 and 0.4 respecitvely). No significant effects for the multivariate heterogeneity of variances were found at any of the stations, indicating homogeneity of variances between seasons (Table 2, **Fig. S2**).

3.3. Seasonal and spatial patterns in functional diversity of macrofauna communities

No significant seasonal differences were observed for functional richness (FRic), functional evenness (FEve) and functional dispersion (FDis). FRic and FDis followed a similar pattern across stations, presenting higher values at the shelf and slope stations compared to the basin stations (Fig. 8**A and C**). FEve increased gradually in variability among replicates for the deep stations (Fig. 8**B**). The functional redundancy at the slope and shallow stations was higher than at the basin stations indicated by low FRed values (Fig. 8**D**). Significant seasonal differences were found at station P2, with significantly higher values in August compared to March and May, and lower values in March than in May, indicating that samples from March had higher functional redundancy. Seasonal differences were also found at station P7, with significantly lower values in March compared to August, indicating again higher functional redundancy in March. Linear regressions between functional diversity (FDis) and H' for all stations and seasons showed significant but not very strong linear relationships (R^2-adjusted = 0.63, p-value= <2e-16 ***) (**Fig. S4**) Relationships were maintained constant

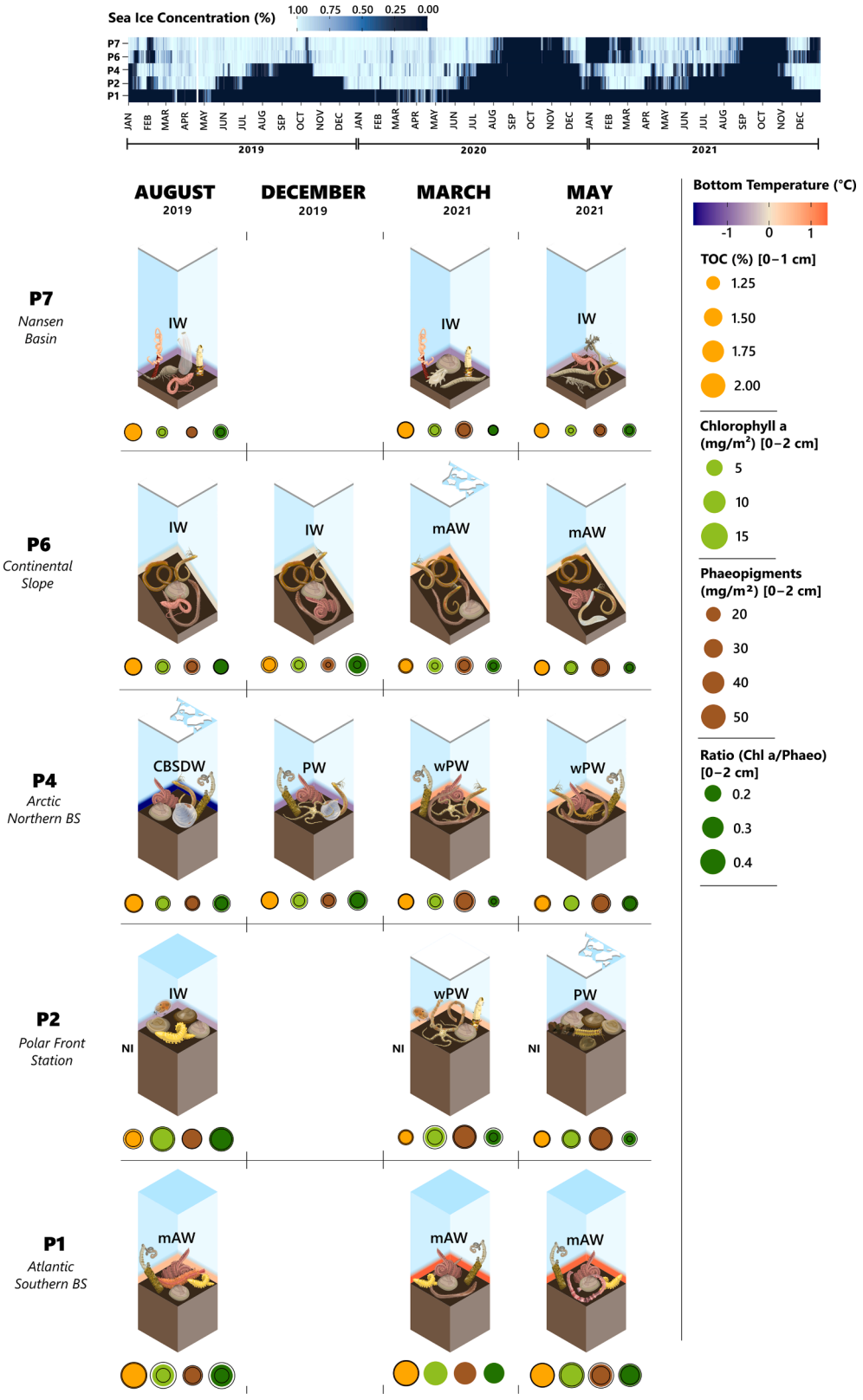

Fig. 3. Overview of some of the most relevant environmental variables varying across stations and seasons. On the top, daily sea ice concentrations from 2019 to 2021 are shown to assess qualitatively the sea ice conditions during the gap year (2020). Bottom water temperatures are shown with color ranging from dark blue to red on top of the seafloor for each station/season (for values see color scale). Bottom water masses are indicated as in Fig. 2. Mean values of sediment pigments (Chlorophyll a and Phaeopigments) and TOC% are shown as colored circles at the bottom of each station/season. Sizes scales represent values and the two black circles around them signify the standard deviation of the mean. Five most abundant taxa for each station/season are shown (for taxa names see Fig. 5 and Table S3).

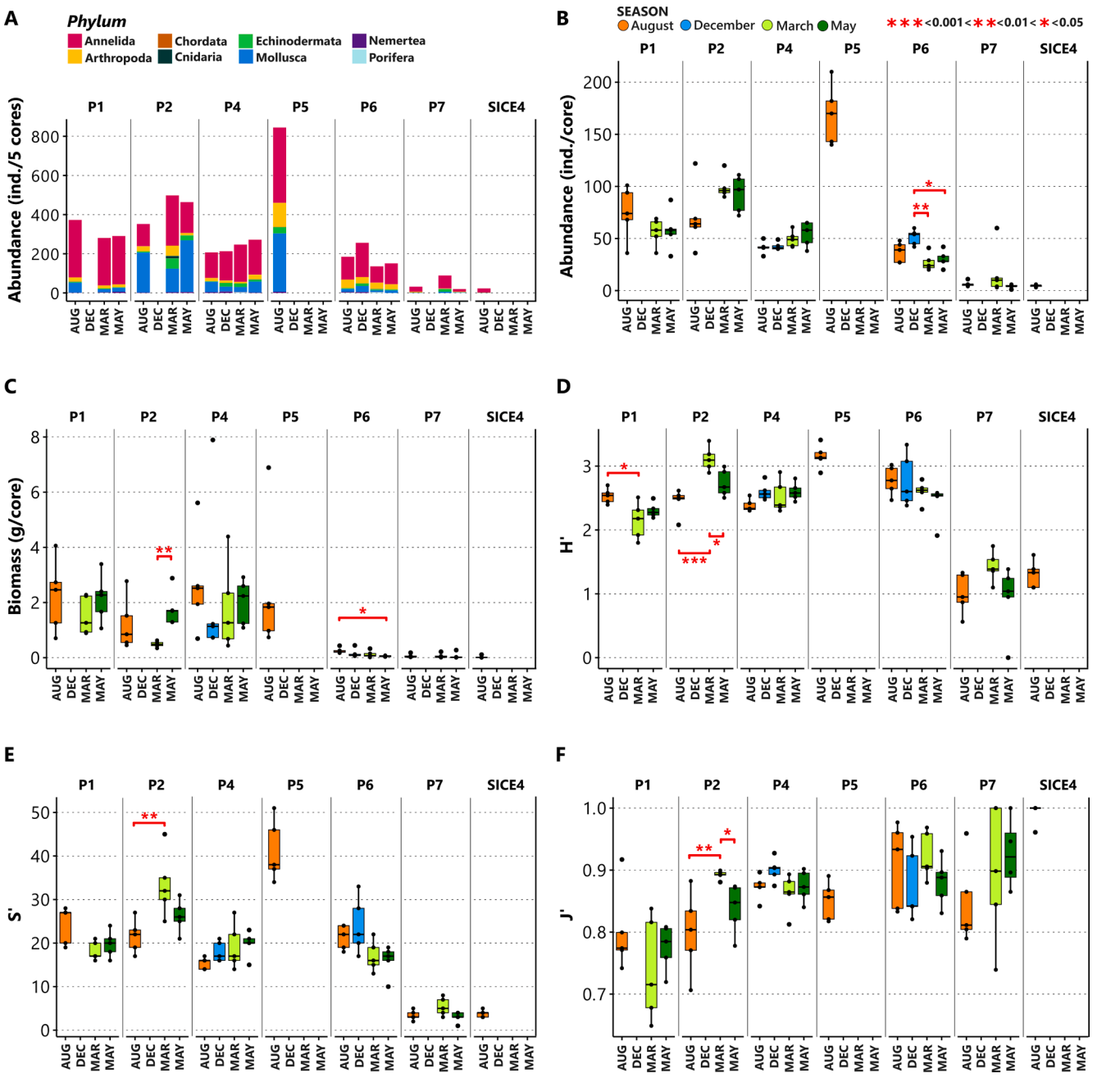

Fig. 4. Macrobenthic community composition and diversity indices from the northern Barents Sea across four seasons from five macrofauna core replicates. A) Stacked bar plots showing abundances of macrobenthos (five replicates pooled) by phylum; B) boxplots for total abundances of macrofauna (significance tests are shown for the square root transformed biomass), C) boxplots for total biomass of macrofauna D) H' (Shannon Index), E) S' (Species richness), F) J' (Pielou Evenness) for each station and season based on abundance. Significant differences in pair-wise comparisons at each station across seasons after the Kruskal-Wallis test and Conover test applying the Bonferroni correction for adjusted p-values are reported in red with asterisks. * $p \leq 0.05$, ** $p \leq 0.01$, *** $p \leq 0.001$. In boxplots, the colored rectangles indicate the interquartile range, which is divided into the upper and lower quartiles by the median (indicated with a black line); whiskers indicate the maximum and minimum values, excluding outliers.

across seasons, except for December due to lack of samples at some stations for that season.

The fuzzy correspondence analysis (FCA) did not show clear groupings across seasons (Fig. 9). Instead, it showed a rather spatial grouping along the first axis (explaining 33.03 % of the variation) differentiating the shelf and slope stations from the P7 station. At the same time, the slope station grouped further apart from the shelf stations along the second axis (which explained 19.56 % of the variation). Trait categories: tube-dwelling (LH3), sessile (MV1), vermiform (BF2), infaunal (EP1), parasite/commensal/symbiotic (FH6) and medium and small/medium (S3 and S2) were positively correlated with samples of P7 along the first axis. In contrast, trait categories for burrower and burrowing (MV2 and LH4), dorso-ventrally and laterally compressed (BF3 and BF4), swimmer and crawler (MV4 and MV3) and small (S1) correlated positively with most shelf station communities, especially at P2. Along the second axis, trait category indicating benthic/direct larval development (LD3) correlated positively with samples of station P6, while pelagic/planktotrophic larval development (LD1) correlated with samples from stations P1 and P2.

The PERMANOVA analysis conducted on the CWM trait matrix

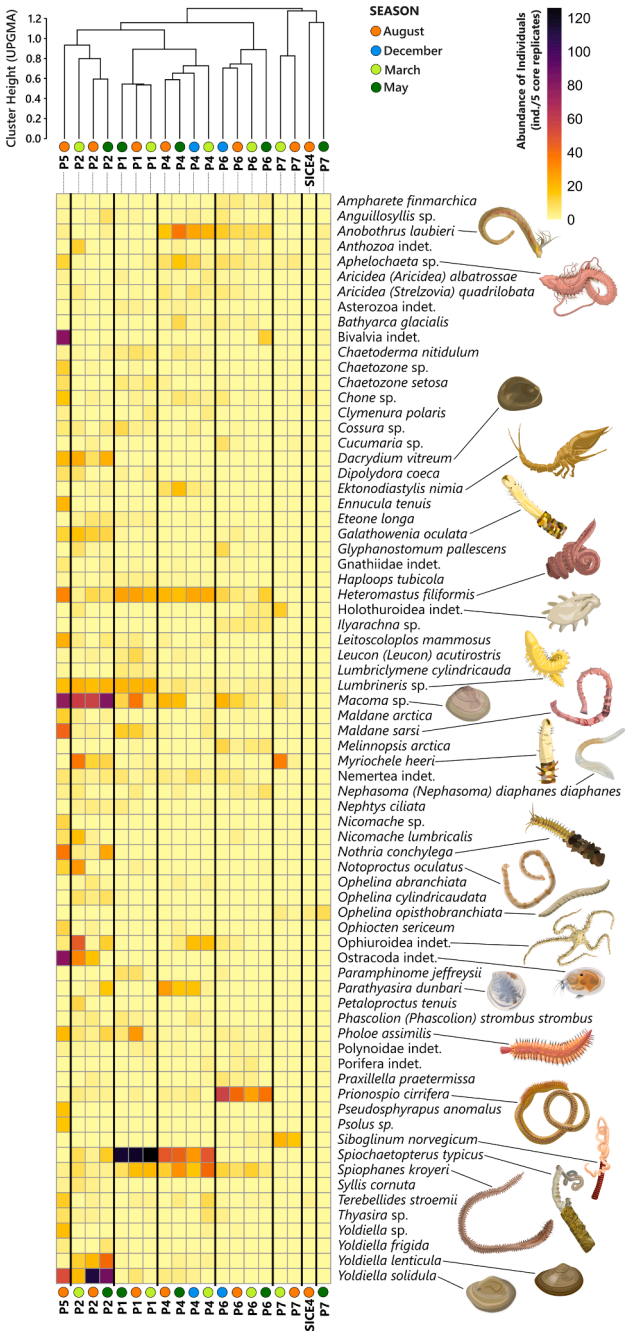

Fig. 5. Cluster dendrogram (UPGMA) based on Euclidean dissimilarity distances calculated from Hellinger transformed macrofauna abundance for the five pooled core replicates for each season (August, December, March and May) and station (P1, P2, P4, P5, P6, P7 and SICE-4). Heatmap shows the raw abundances of the most abundant taxa (>10 individuals in total for all summed samples of the entire study) are shown below the cluster analysis. Macrofauna abundance values are shown for the five pooled core replicates at each station/season (see color scale on the top right). Drawings for some of the most abundant species are presented. *D. vitreum*, *Macoma* sp., *P. dunbari* and *Y. lenticula* are redrawn from images © Amgueddfa Cymru – National Museum Wales using Inkscape. *H. filiformis* is redrawn from image © Fredrik Pleijel using Inkscape. *N. diaphanes* is redrawn from © "Nephasoma diaphanes" - Nephasoma diaphanes (Gerould, 1913) collected in United States of America by Florida Museum of Natural History Invertebrate Zoology (licensed under http://creativecommons.org/licenses/by-nc/4.0/). All drawings made by Èric Jordà Molina with Inkscape 1.3 (0e150ed6c4, 2023–07-21). Drawings are just for illustrative purpose and are not made to taxonomic detail.

considering all stations and seasons (Table 3) identified statistically significant differences between stations ($R^2 = 0.33$), seasons ($R^2 = 0.04$) and the interaction of station and season ($R^2 = 0.12$). When taking each station individually into account, significant seasonal differences were found at station P2 (March samples vs. August and May samples). For station P4, significant differences were found between samples collected in August and March, and August and December. Again, station P2 had the highest R^2 for the factor season ($R^2 = 0.49$). No significant effects for the multivariate heterogeneity of variances were found at any of the stations, indicating homogeneity of variances between seasons (Table 3, **Fig. S2**).

3.4. Spatio-temporal variation partition of macrofauna with environmental variables

The variation partition for the macrofauna community composition (Hellinger transformed abundance-based) (Fig. 10**A**) showed that temporal predictors (AEMs 9 and 6, see supplementary material **Fig. S6**) only explained 2 % of the macrofauna variation. Thirty five percent of the variation, in contrast, was explained by the selected environmental variables (in decreasing importance depth, TOC, mean grain size, bottom salinity, bottom temperature, sea ice concentration and sediment phaeopigments) of which 24 % was explained together with the spatial structure (MEM1, 4 and 3). In total, 31 % of variance was explained by the spatial structure.

For the CWM traits dataset (Fig. 10**B**), no AEMs were selected in the forward selection step, and therefore, no variation was attributed to seasonality in macrofauna trait composition. In contrast, environmental variables selected (in decreasing importance: depth, TOC, bottom water salinity, sea ice concentration, mean grain size and bottom temperature) accounted for 29 % of the variation, while the spatial structure (MEM1, 3, 4 and 2) accounted for 26 % of the variation. Of that, 21 % was accounted for by both the environmental variables and spatial structure.

As for the variation partitions at each station (Fig. 11**A,B**), for station P1 the analysis attributed 4 % variation on the abundance based macrofauna dataset to environmental variables (bottom water salinity) and 4 % to the temporal predictors (AEM9). No environmental variables or AEMs were selected for the CWM-based dataset. For station P2, the abundance-based partition attributed 21 % of variation to the environmental variables (bottom water temperature) and 21 % to the selected AEMs (AEM2). For the CWM-based dataset, 39 % of variation was attributed to the environmental variables (bottom water temperature) and 39 % to the temporal predictors (AEM2). For station P4, 12 % of variation was attributed to the environmental variables (chlorophyll *a* and phaeopigments) together with the AEMs selected (AEM4 and 6) for the abundance-based macrofauna, while 6 % of total variation was attributed to the temporal component alone. For the CWM-based dataset, 17 % was attributed to the environmental variables (bottom water salinity) and 18 % to the selected AEMs (AEM4 and 7). At station P6, 8 % and 7 % of variation in the abundance-based macrofauna dataset was attributed to the environmental variables (sediment phaeopigments) and temporal predictors (AEM5) respectively, while no environmental variables were selected for the CWM-based dataset (despite AEM3 being selected after FWS). Lastly, at station P7, 25 % of variation was attributed to environmental variables (bottom water temperature) together with AEMs selected (AEM3 and 1) for the abundance-based dataset, while no variation was explained by either of the explanatory sets alone. No variables were selected for the CWM-based data for that station.

4. Discussion

In shallow temperate coastal environments, macrofauna communities often undergo significant seasonal fluctuations, presenting lower biomass in late winter and an increase in biomass from early summer to early fall (Beukema, 1974; Baird and Ulanowicz, 1989; Zwarts and Wanink, 1993; Coma et al. 2000; Saulnier et al., 2019). This increase in

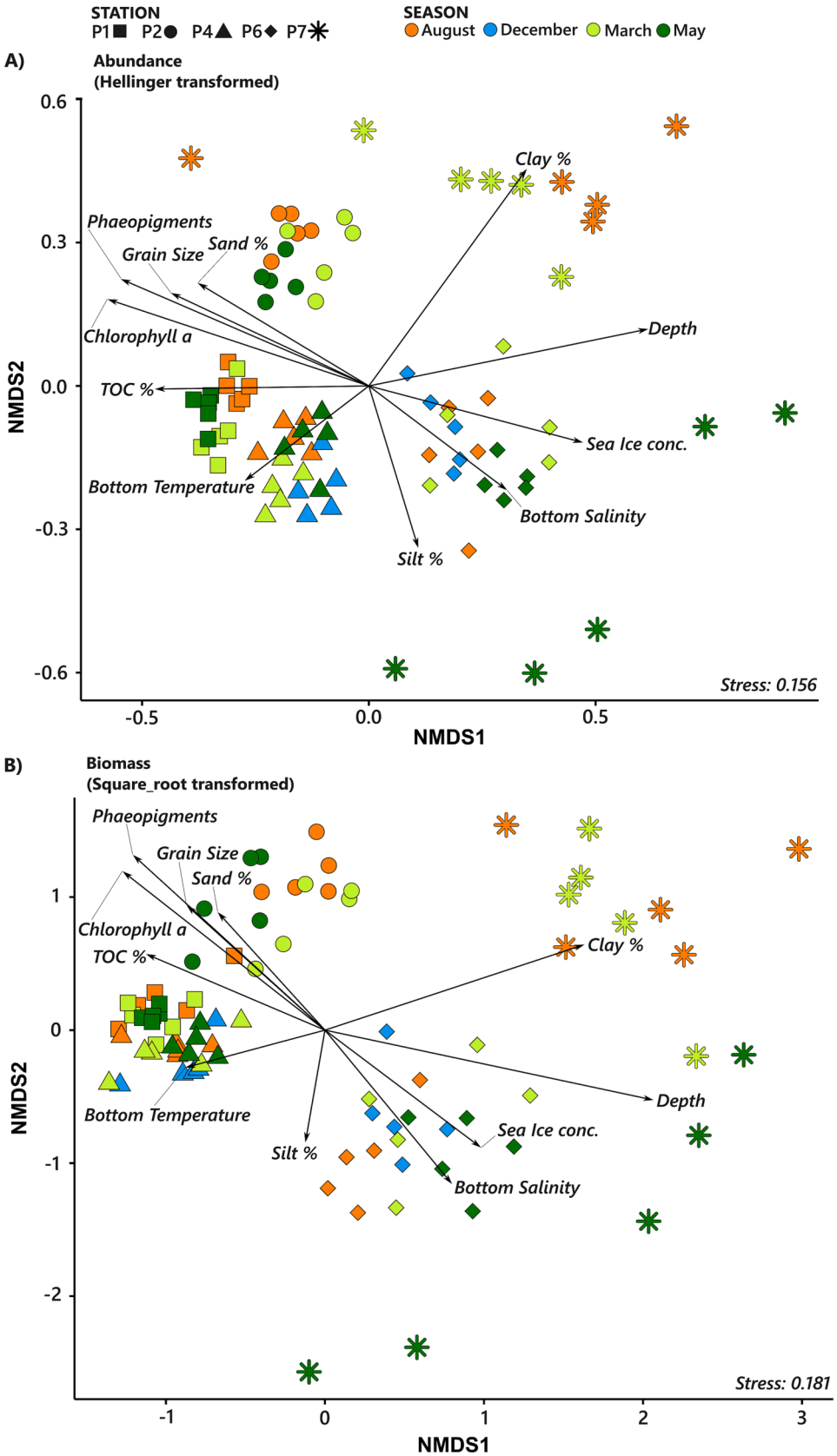

Fig. 6. Non-metric multidimensional ordination (nMDS) showing A) the similarity between sample replicates by season and station of Hellinger-transformed macrofauna abundance data using Euclidean distances, and B) the similarity between replicates by season and station of the square root transformed macrofauna biomass using Bray-Curtis distances from the northern Barents Sea.

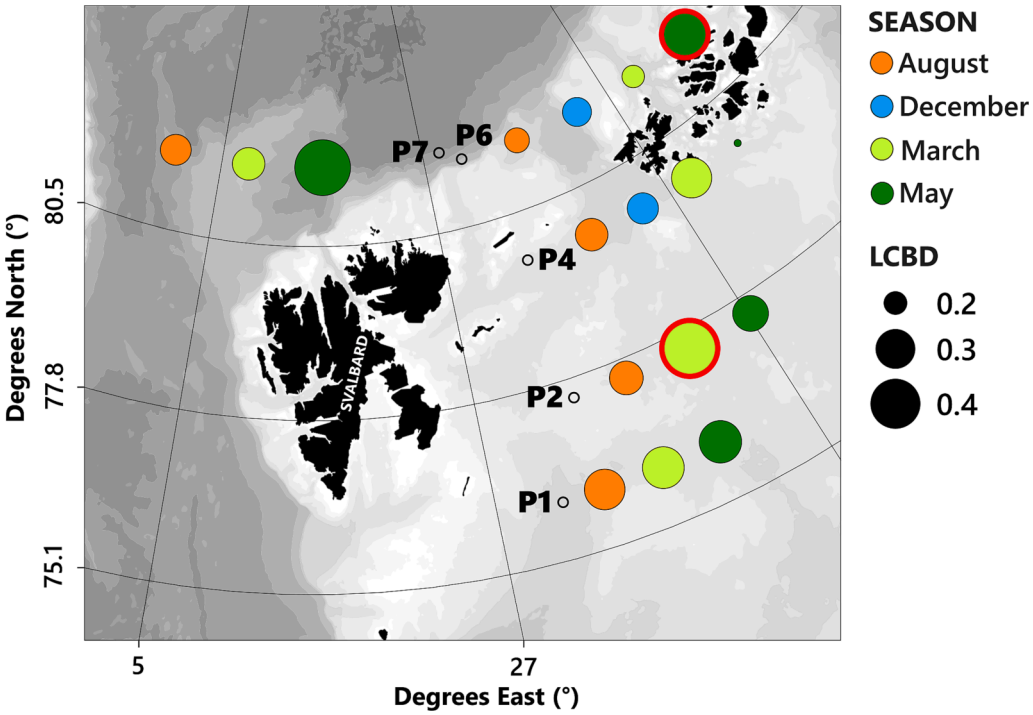

Fig. 7. Map showing the results of the Local contribution to beta diversity (LCBD) for the Hellinger transformed macrofauna abundance in the northern Barents Sea across four seasons. The position of each station is indicated with empty circles. LCBD values for each station across seasons are indicated with colored circles the sizes of which indicate the LCBD value and the color the season. LCBD values are calculated individually for each station comparing seasons and therefore should not be compared between locations. LCBD indices from seasons which are significant are indicated with a red rim (p adjusted-value < 0.05 after applying the Holm correction for multiple testing) indicating seasons that are more unique in community composition than the average composition of the other seasons.

biomass during summer coincides with increasing temperatures, primary production and food availability to the seafloor, which induces an increased somatic growth and is accompanied by recruitment pulses (Reiss and Kröncke, 2005; Saulnier et al., 2019). On the contrary, the lower food supply during winter could be the reason behind weight loss and, together with increased predation pressure, increased natural mortality (Saulnier et al., 2019). These seasonal patterns in temperate environments, however, may differ from equatorial or polar regions with little or extreme seasonality in environmental conditions, respectively (Saulnier et al., 2019).

High Arctic marine ecosystems are characterized by marked seasonal pulses of primary production and fluctuations in abiotic parameters (i.e. seasonal sea ice cover, among others) which constrain the phenology, structure and composition of pelagic communities (Daase et al., 2013; Søreide et al., 2013). Hence, assuming that the Barents Sea is a tightly pelagic-benthic coupled system (Wassmann et al., 2008; Wassmann and Reigstad, 2011), we hypothesized that benthic standing stocks (i.e. macrofauna) might reflect seasonal patterns in their taxonomic and functional composition that mirror those in the overlying water. Conversely, the results of our study indicate a general lack of seasonality in macrobenthic community parameters, and especially, in functional composition (Fig. 10). We found only weak seasonal patterns at some individual stations with respect to the others, indicating that, any seasonality is site-context specific along the northwestern Barents Sea and adjacent Nansen Basin, a region comprising different sea ice, hydrographical and productivity regimes and extending over different geomorphological settings (shelf, slope and deep basin). We also hypothesized that seasonal patterns, if present, might be driven by seasonal fluctuations in sea ice cover, water mass properties and food availability. Although we found seasonal variations in some environmental parameters within stations (in fact environmental variables where highly spatially structured), no pronounced seasonal variations were observed across the whole region for bottom water properties (except at P2 and P4) and food availability, indicating relatively stable seafloor conditions year-round. In particular, total organic carbon in surface sediment (and to some extent sediment pigments) remained seasonally stable at all stations, pointing towards a decoupling of seafloor food availability from seasonal pelagic food export to depth.

Given that no extreme differences were found between seasons from differing years (2019 and 2021) in both taxonomic and functional composition and that most sediment parameters remained relatively stable in most cases, we consider that treating the two years over which the study was conducted as if they were consecutive, reflecting a full annual cycle, is a valid approach to discuss the results of our study.

4.1. *Lack of seasonality in macrofauna and similarity in macrofauna on the shelf on either side of the Polar Front*

Station P1, south of the Polar Front, did not show strong signs of seasonal variability in either taxonomic or functional composition. This station is Atlantic Water (AW) influenced with year-round presence of modified Atlantic Water (mAW) bottom water masses and consistent open-water conditions. Here, we observed some environmental variability driven mainly by small increases in chlorophyll *a* and phaeopigments in the sediments, and in bottom water temperatures in March and May compared to August, while sediment variables such as TOC remained relatively constant across seasons (Ricardo de Freitas et al., 2023 under review) (Figs. 2 and 3, **Table S2**). Consequently, the environmental variables did not seem to play a major role in driving macrofauna variation across seasons (Fig. 11). Station P4, north of the Polar Front and with high sea ice cover, also lacked seasonal differences in univariate taxonomic and functional metrics, and low variance explained by seasons in species and trait composition despite some significant seasonal differences in community composition (Tables 2 and 3). It is important to bear in mind that the PERMANOVA analyses are taking into account the whole community including the rare species, and

Table 2
PERMANOVA results from the macrofauna community abundance Hellinger-transformed. Results from a two-way model including all stations and all seasons (and interaction) and one-way models for each station separately across the different seasons. Stations with samples in only one season were not included (P5 and SICE-4). P-values from post-hoc pair-wise comparisons were corrected with the Bonferroni method and only significant comparisons are reported. Df = degrees of freedom, R^2 = adjusted R^2, F = F-statistic, Pr(>F) = p-value. The test of homogeneity of multivariate dispersion (Betadisper) is shown for each station for the season factor. Df = degrees of freedom, F = F-statistic and Pr(>F) = p-value from the test are reported.

		Df	R^2	F	Pr(>F)	Pair-wise Comparison (only station by station)
All						
	Station	4	0.39	15.75	**1e-04** ***	
	Season	3	0.05	2.72	**1e-04** ***	
	*Station*Season*	9	0.13	2.35	**1e-04** ***	
	Residuals	68	0.42			
P1						
	Season	2	0.20	1.53	**0.0049** **	August vs May *
						March vs May *
	Residuals	12	0.80			
	Betadisper	2		0.15	0.860	
P2						
	Season	2	0.42	4.38	**1e-04** ***	August vs March **
						August vs May **
	Residuals	12	0.58			March vs May **
	Betadisper	2		0.85	0.447	
P4						
	Season	3	0.34	2.83	**1e-04** ***	August vs December **
	Residuals	16	0.65			August vs March **
						August vs May **
						December vs March **
						December vs May **
						March vs May **
	Betadisper	3		0.754	0.531	
P6						
	Season	3	0.25	1.81	**5e-04** ***	August vs May **
						December vs March **
	Residuals	16	0.75			December vs May **
						March vs May *
	Betadisper	3		2.49	0.100	
P7						
	Season	2	0.40	3.97	**2e-04** ***	August vs March *
						August vs May **
	Residuals	12	0.60			March vs May **
	Betadisper	2		0.145	0.876	

significant differences could be reflective of sampling size limitations to effectively account for the rare fraction of specimens, yielding significant differences across seasons. Interestingly, this station had similar macrofauna taxonomic composition to station P1 (Figs. 5 and 6**A**). At both stations, the spiochaetopterid polychaete *S. typicus* dominated in abundance. This species has boreal biogeographic affinities (Bhaud, 1998), high tolerance to environmental disturbance and dual surface deposit and filter/suspension feeding modes (Degen and Faulwetter, 2019). This might be an indication that P4 is influenced by AW advective processes, with higher bottom water temperatures and food availability (either in-situ or advected). Lundesgaard et al. (2022) observed intrusions of the Arctic Circumpolar Boundary Current, flowing along the slope, into the northern Barents Sea shelf through the Kvitøya and Franz Victoria Troughs, flowing southwards and converging around our P4 station (Fig. 1). This is supported by the signs of wPW in March and May that we observed in this station, which is likely a product of AW or mAW that has been mixed with PW (Sundfjord et al., 2020). Whether the similarity in faunal assemblages is driven by bottom thermal preferences, larval advection or food availability is difficult to conclude. Benthic communities in the Barents Sea are in fact highly constrained by the spatial extent of bottom water masses, particularly of AW (Carroll et al., 2008; Cochrane et al., 2009). Hence, it appears from our results that AW-influenced bottom water regions along the northwestern Barents Sea shelf displayed the least seasonal fluctuations in macrofauna communities despite presenting spatially distinct sea ice cover and seafloor food availability.

4.2. *Weak signs of seasonality in macrofauna at the Polar Front*

Macrofauna communities at station P2 showed the strongest seasonal signals in community composition compared to all other stations along the transect, which was also reflected in functional composition (Fig. 11 and Table 2, 3). While fine-scale temporal patterns in macrofauna variation at P2 were not selected to explain any variation on the macrofauna data (Fig. 11 **and S6**; i.e. month to month variability, which do not fit with expected phenological dynamics in the water column), both macrofauna taxonomic and functional fluctuations were partially explained by longer time-scale predictors (i.e. AEM_2 Fig. 11), mirroring expected seasonal patterns at these latitudes for water column processes. In general, significant increases in species diversity, richness and evenness were observed from August to March (with more unique taxonomic composition in the latter), followed by general significant decreases in May (Fig. 4). It is well known that in areas with overlaying oceanographical fronts, sea ice edge and polynya areas (such as the Barents Sea Polar Front) macrobenthic species diversity and density is enhanced (Wassmann et al., 2006; Carroll et al., 2008; Cochrane et al., 2009). This was also the case in our study along with the strongest seasonal variations in environmental parameters observed at station P2. For instance, sea ice cover was highly variable together with bottom water masses and, to a certain extent, chlorophyll *a*, phaeopigments and food quality ratios (Fig. 3, **Table S2**). Hence, this station is likely under the influence of the transitional area of the Polar Front, separating both Atlantic and Arctic domains with high seasonal variability in its oceanographic dynamics. This might result in a tighter pelagic-benthic coupling (Carmack and Wassmann, 2006; Cochrane et al., 2009), in which short pulses of high quality food (rather than the overall productivity of the water column) might be of high importance for benthic community structure. However, seasonal differences in macrofaunal taxonomic and functional composition at P2 were better explained by bottom water temperature instead of any food availability proxies. In this station, we found signs of bottom wPW in March, indicating a certain degree of Atlantic advection, but macrofauna community composition was different from the highly Atlantic influenced stations P1 and P4 with surface deposit feeding bivalves (*Macoma* sp. and *Y. solidula*) dominating at P2 (Fig. 5). This distinction in macrofaunal assemblages may arise from the difference in depth and in sediment granulometry between stations, since P1 and P4 were located in troughs with finer sediment grain sizes, while P2 was located in the Storebankken bank, with coarser grain sizes (Fig. 1). This is supported by the similarity in fauna composition of P2 with P5, as the latter was also located in a shallow bank next to Kvitøya, even though we only had data for one season (Fig. 5).

The increase in abundances of several polychaete species (i.e. *Myriochele heeri*, *Nicomache lumbricalis*, *Notoproctus oculatus)* and Ophiuroidea indet. in March at P2 could be due to recruitment into the community (bearing in mind that effects of recruitment in adult populations would be due most likely to recruits from the previous year, since most small recruits would be lost at the mesh sizes that we sieved our samples) (Fig. 5). The life cycles of the polychaeta families these species belong to, oweniids and maldanids, have maximum larval occurrence and posterior recruitments around the spring bloom in Arctic waters (Fetzer and Arntz, 2008), which was also observed by Włodarska-Kowalczuk et al. (2016), who found seasonal differences in the size of oweniid polychaetes in Kongsfjorden.

From our data, however, it is not possible to infer any recruitment

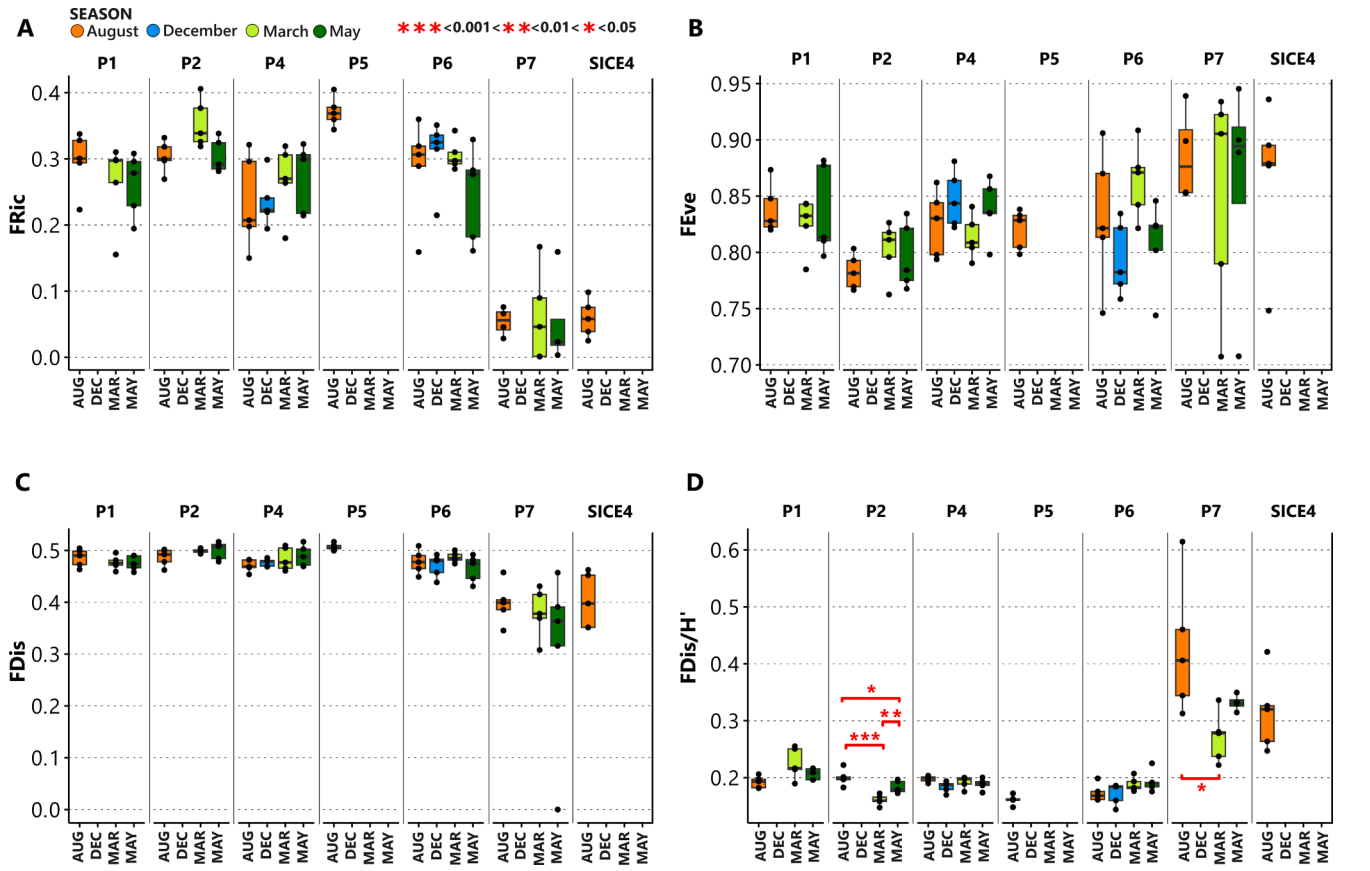

Fig. 8. Boxplots for functional diversity indices of macrofauna traits from Hellinger transformed abundances in the northern Barents Sea across seasons. A) FRic (Functional richness), B) FEve (Functional evenness), C) FDis (Functional dispersion), D) FRed (Functional redundancy ratio = FDis/H', low ratio indicates high functional redundancy). Significant differences in pair-wise comparisons at each station across seasons after the Kruskal-Wallis test and Conover test applying the Bonferroni correction for adjusted p-values are reported in red with asterisks. * $p \leq 0.05$, ** $p \leq 0.01$, *** $p \leq 0.001$. In boxplots, the colored rectangles indicate the interquartile range, which is divided into the upper and lower quartiles by the median (indicated with a black line); whiskers indicate the maximum and minimum values, excluding outliers. Black dots indicate the values of for the different replicates.

patterns, since we did not measure individual sizes and we missed juveniles smaller than our mesh size (0.5 mm) (Mincks and Smith, 2007). However, no distinct recruitment events were evident in our data based on visual observation of macrofauna sizes (e.g. no clear juvenile cohorts were observed in the samples). Also, preliminary results from analysis of biomass size spectra of the macrofauna samples from our study suggest a rather lack of seasonal pulses in the sizes of bigger recruit fractions, only showing relatively stronger variations between seasons at station P2 (Barbara Górska, personal communication in July 2023). Studies from the West Antarctic Peninsula (WAP) have shown that most polychaete species displayed marginally seasonal to non-seasonal patterns of recruitment as indicated by the year-round presence of small juveniles for most macrofaunal taxa (Glover et al., 2008; Mincks and Smith, 2007). Due to this apparent decoupling of recruitment from pelagic processes, direct and lecithotrophic larval development modes seem to be selected rather than the planktotrophic ones in the WAP (Smith et al., 2006). In fact, the dominant larval development in our study was direct benthic larval development, while planktotrophy (LD1) was usually under 40 %. This could support the theory that benthic recruitment processes might be highly decoupled from pelagic bloom phenology in the Barents Sea, and rely mainly on constant food availability to sustain reproduction activities and dispersal/recruitment processes year-round. In a similar line, Descôteaux et al. (2021) identified a clear mismatch between meroplankton bulk abundance peaks and phytoplankton bloom occurrence in the Barents Sea. However, they found that most larvae in the meroplankton bulk were planktotrophic, suggesting that perhaps these larval modes might feed on other sources than the dominant diatoms during the peaks of primary production (Cleary et al., 2017; Descôteaux et al., 2021). Therefore, it is possible that food availability might be an important driver for recruits in this area of the Barents Sea, and that its potential seasonal constancy in the surface sediments might translate into constant pulses of successful recruitments year-round (despite taxon specific differences in timing of reproductive cycles).

4.3. *"Seasonal" differences at the deep stations could be due to spatial heterogeneity or inter-annual changes*

Apart from station P2, the northernmost stations at the continental slope (P6) and in the Nansen Basin (P7) also showed some temporal variations in taxonomic composition (Figs. 7 and 11 **and** Table 2). This could be attributed to the fact that the area around the continental slope and adjacent parts of the Nansen Basin act as a highly dynamic polynya, as the warm circumpolar boundary current flows along the slope north off Svalbard, melting the sea ice (Lundesgaard et al., 2022). This creates zones of frequently open waters with higher seasonal productivity (Falk-Petersen et al., 2015), strong advection processes from further south, and perhaps tighter pelagic-benthic coupling interactions. Dybwad et al. (2022) suggested that vertical fluxes of total particulate matter (TPM) and TOC along the northern slope of Svalbard is higher towards the west where sea ice cover increases gradually and the AW gets mixed along the slope and enters into the Arctic Ocean. However, they observed a greater mismatch between the spring blooms and the grazer communities towards the east of the slope, close to our P6 and P7 stations, indicating more rapid exports of primary production blooms to depth despite their

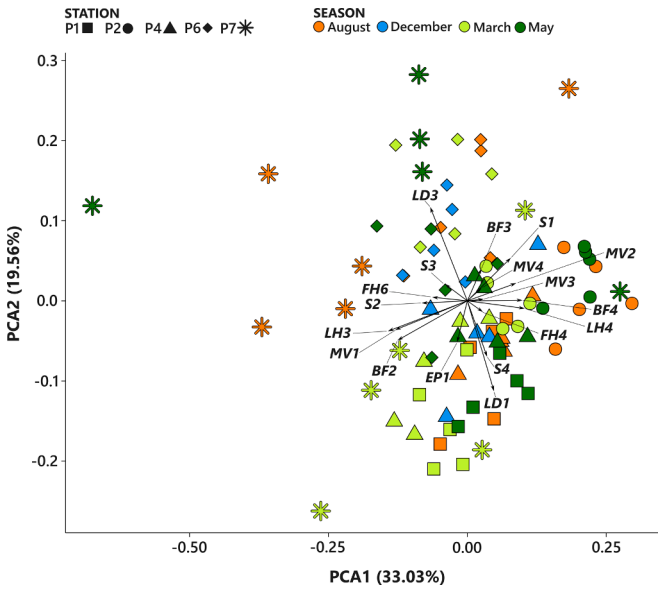

Fig. 9. Fuzzy Correspondence Analysis showing the contribution of trait categories in correlation to the seasonal and spatial (stations) functional structure based on the community weighted means of trait composition of Hellinger transformed abundances. Only trait categories with Pearson correlations higher than 0.5 with either the first or second axis are shown in the vectors. S1 = Small (<10 mm); S2 = Small-medium (10–50 mm); S3 = Medium (50–100 mm); S4 = Medium-large (100–300 mm); BF2 = Vermiform, elongate; BF3 = Dorso-ventral compressed; BF4 = Laterally compressed; LH3 = Tube dwelling; LH4 = Burrowing; MV1 = Sessile/none; MV2 = Burrower; MV3 = Crawler; MV4 = Swimmer (facultative); LD1 = Planktotrophic larval development; LD3 = Direct/benthic larval development; FH4 = Opportunist/Scavenger; FH6 = Parasite/Commensal/Symbiotic; EP1 = Infauna.

lower total bulk.

The sea ice concentration values along the transect from the beginning of 2019 and into 2021, indicated that the polynya around P6 and P7 was of an inter-annual intermittent character, since stations P6 and P7 were generally ice-free around January and February of 2019 and 2021, but were almost completely ice covered in 2020. The fact that no polynya developed in 2020 and that we sampled macrobenthic communities only in 2019 (August and December) and 2021 (March and May) could be one of the reasons why we see more striking differences in the communities (i.e., abundance, biomass and species richness) between these two periods (and perhaps could be more indicative of inter-annual fluctuations). However, the environmental variables at the slope (including sediment pigments and TOC), and in the adjacent basin did not differ substantially across seasons. It is also important to notice that station P6, was at slightly different locations between seasons and the rapid changes in depth due to difficulties to maintain the ship's position in strong sea ice drifting conditions. This might have caused sampling slightly different geomorphological conditions in this heterogeneous environment (Kollsgård et al., 2021), with potentially differing macrofaunal communities associated with it. At P7 the low faunal densities in the deep sea and the resulting high small-scale variability (Gallucci et al., 2009; Rex and Etter, 2010; Vedenin et al., 2016), in combination with relative small sample sizes of our study, might have increased the risk for mistaking small spatial differences for seasonal differences in community structure (compared to the shelf stations). This was reflected in the nMDS, were replicates at the deepest stations were more dissimilar to each other in community composition compared to the replicates from the shelf. Therefore, the "seasonal" differences found for these two stations should be considered with caution. Nevertheless, we want to stress again that all these seasonal differences (although significant in some cases when analyzing each station separately) were small when looking at the whole regional scale of the study area.

Table 3
PERMANOVA results from the community weighted means (CWM) from the macrofauna functional traits weighted by the Hellinger-transformed abundances. Results from a two-way model including all stations and all seasons (and interaction) and one-way models for each station separately across the different seasons. Stations with samples in only one season were not included (P5 and SICE-4). P-values from post-hoc pair-wise comparisons were corrected with the Bonferroni method and only significant comparisons are reported. Df = degrees of freedom, R^2 = adjusted R^2, F = F-statistic, Pr(>F) = p-value. The test of homogeneity of multivariate dispersion (Betadisper) is shown for each station for the season factor. Df = degrees of freedom, F = F-statistic and Pr(>F) = p-value from the test are reported.

		Df	R^2	F	Pr(>F)	Pair-wise Comparison (only station by station)
All						
	Station	4	0.33	10.80	**0.0001** ***	
	Season	3	0.04	1.78	**0.0**308 *	
	*Station*Season*	9	0.12	1.79	**0.00**16 **	
	Residuals	68	0.51			
P1						
	Season	2	0.22	1.67	0.0635	*March vs May * (p = 0.04)*
	Residuals	12	0.78			
	Betadisper	2		0.20	0.829	
P2						
	Season	2	0.49	5.84	**0.000**6 ***	August vs March ** March vs May **
	Residuals	12	0.51			
	Betadisper	2		1.36	0.299	
P4						
	Season	3	0.32	2.56	**0.00**24 **	August vs December *
	Residuals	16	0.68			August vs March **
	Betadisper	3		0.35	0.783	
P6						
	Season	3	0.21	1.45	0.145	
	Residuals	16	0.79			
	Betadisper	3		0.60	0.623	
P7						
	Season	2	0.20	1.53	0.161	
	Residuals	12	0.82			
	Betadisper	2		0.60	0.597	

4.4. Lack of macrofauna seasonality through constant food availability (food bank)

Benthic surface sediment pigment concentrations are known to be a good proxy for water column productivity and have been shown to influence benthic community structure and function in Arctic shelves (Ambrose and Renaud, 1995; Piepenburg et al., 1997; Cochrane et al. 2009). Chlorophyll *a* gives an indication of the "freshness" of the organic matter reaching the seafloor, as it is directly derived from pelagic primary production exported to depths (Boon and Duineveld, 1996) having a few-week-long half-life in polar sediments (Renaud et al., 2008). On the other hand, phaeopigments are a result of degradation products from fresher organic matter that have been through degradation processes (such as pelagic grazing), which accumulate in surface sediments over longer temporal scales than chlorophyll *a* (Morata and Renaud, 2008). The pulsed and highly seasonal nature of primary production in the high Arctic would suggest that a similar seasonal pattern should be expected in food availability to the seafloor realm. Of course, the magnitude in the amount of OM reaching the ocean floor through vertical flux will depend, among others, on bacterial degradation and grazing activities by planktonic organisms, but we would expect that the temporal patterns would be similarly translated into the seafloor sediments when it comes to what is available for fueling benthic standing stocks. Nevertheless, pigment concentrations (although displaying spatial differences between stations) remained relatively stable across seasons, especially

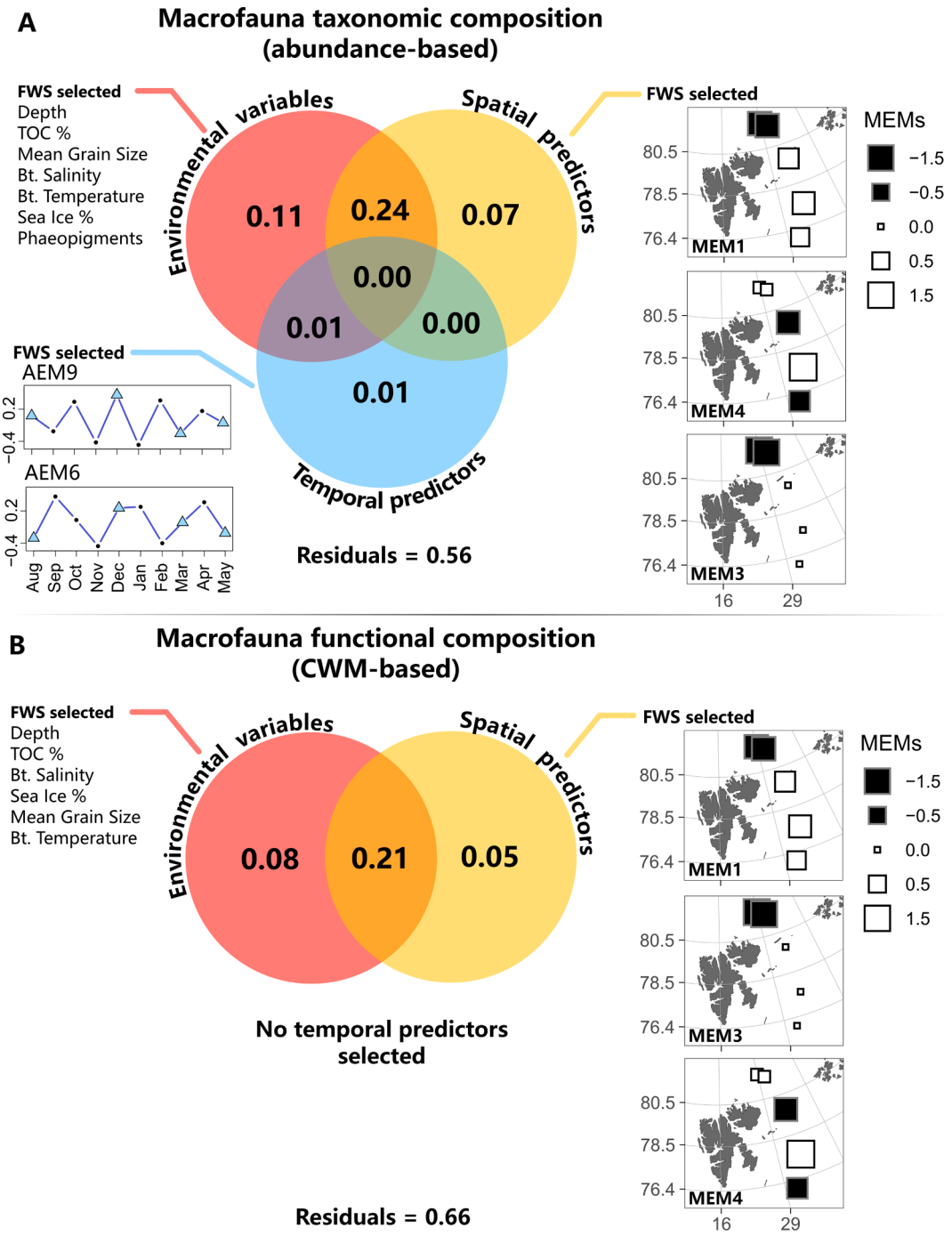

Fig. 10. Venn diagrams showing the variation partition of the temporal structure (Asymmetric Eigenvector Maps. AEMs) (blue circle), environmental variables (pink circle), spatial structure (Mooran Eigenvector Maps. MEMs) (yellow circle) and that contributes to explain the macrofauna taxonomic composition (A) and macrofaunal functional composition (CWM) (B) respectively. stations P5 and SICE4 were excluded. Next to each circle the variables that were selected after forward selection (FWS) are shown. The spatial predictors are shown as Moran eigenvector maps (MEMs) (with axis in degree north latitude and east longitude units) and each square represent a station (P1, P2, P4, P6 and P7 from south to north). Size of the squares are proportional to the scores of the eigenvectors and the color shows the sign of autocorrelation among sites (black, negatively correlated and white, positively correlated). For the temporal predictors, AEMs are shown as decomposed sine waves, with months on the x axis and eigenfunction scores in the y axis. Blue triangles represent sampling dates while black dots are the dummy dates included to construct AEMs due to irregular time intervals of sampling (see methods section for detailed explanation).

for chlorophyll *a*. Also other indicators for high-quality OM such as C:N ratio (Ricardo de Freitas et al., 2023, under review this issue) and, to a lesser extent, phaeopigment content remained relatively constant throughout the seasons (Fig. 3 and **Table S2**). This lack of seasonally fresh OM input to the benthos could be due to intensive grazing activities in the water column, resulting in most of the input to the seafloor being in form of phaeopigments (Morata and Renaud, 2008). In fact, there was quite a strong development of grazing communities around spring and summer in stations north of the Polar Front, as Bodur et al. (2023) (in this issue) measured high amounts of fecal pellet derived carbon with sediment traps down to 200 m, indicating high grazing and degradation of fresh OM during the productive season.

Another possible explanation is that macrobenthic communities from the northern Barents Sea, which are hypothesized to be food-

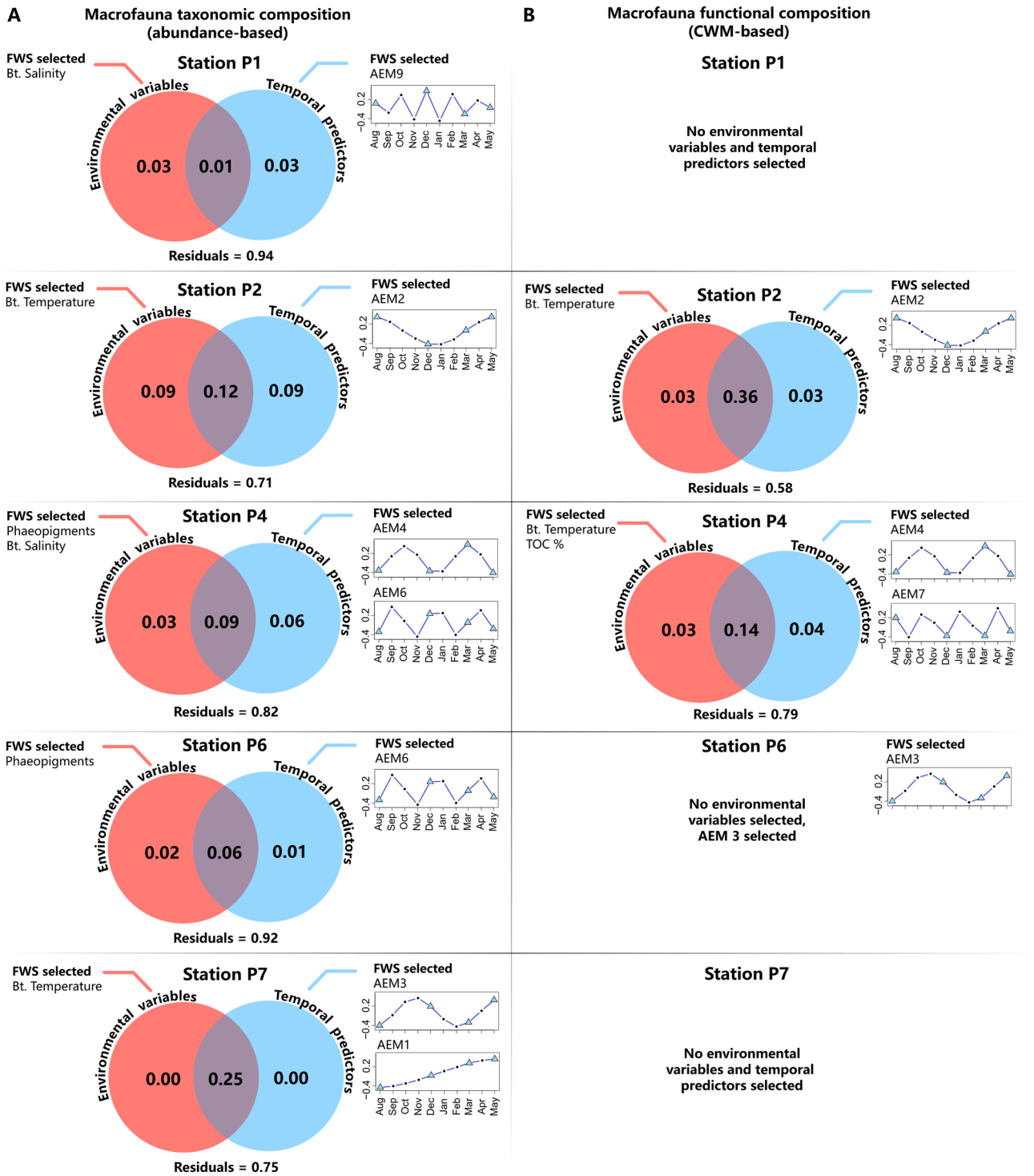

Fig. 11. Venn diagrams showing the variation partition of the temporal structure (Asymmetric Eigenvector Maps. AEMs) (blue circle) and environmental variables (pink circle) and that contribute to explain the macrofauna taxonomic composition and (B) macrofaunal functional composition (CWM) respectively. Variations partitions are conducted for each station individually, and therefore no spatial predictors (Mooran Eigenvector Maps. MEMs) are included. For the temporal predictors, AEMs are shown as decomposed sine waves, with months on the × axis and eigenfunction scores in the y axis. Blue triangles represent sampling dates while black dots are the dummy dates included to construct AEMs due to irregular time intervals of sampling (see methods section for detailed explanation).

limited (Cochrane et al., 2009 and experience lower overall productivity, process and utilize the fresh sporadic pulses of OM reaching the seafloor very efficiently (Morata et al., 2015), hampering its detection in surface sediment. The two most dominant feeding habit modes across the whole transect were sub-surface deposit feeders and suspension/filter feeders, followed, by sub-surface deposit feeder (**Fig.S3**). Carroll et al. (2008) argued that despite the high bioturbation potential of the surface and sub-surface deposit feeding types, the mixing activities of the seafloor fauna in this region of the Barents Sea are much lower compared to those of other continental shelves, and that this leads to low intensity of sediment mixing and shallow mixed depth in the sediments. Ricardo de Freitas et al. (2023, under review this issue) observed almost no variation in TOC across the sediment profiles for the first 5 cm of sediment surface for the same stations of our study, nor seasonal

variations for the sediment profiles. Sediment surface OM could therefore be more prone to resuspension, given the occurrence of strong bottom water currents originated by brine rejection in ice-covered areas of the Barents Sea during late autumn (Årthun et al., 2011), which create a distinctive nephloid layer that transports organic matter across the Barents Sea and even injects it into the deeper Arctic Ocean basin (Buettner et al., 2020; Rogge et al., 2023). Therefore, resuspension processes could be another reason why we did not detect high seasonal differences in the concentration of sedimentary phaeopigments. Instead, the constant levels of bulk TOC, which integrates sediment pigments and many other sources of OM, could be the basis for the lack of seasonal patterns observed at this and the other highly advective stations of this region (P1 and P4). This is supported by the lack of variability in food web structure of benthic communities observed in the same locations and seasons by Ziegler et al. (2023), this issue, who found that communities relied consistently on degraded OM, most likely of resuspended origin.

So far, studies on the seasonality of polar benthic communities have yielded diverging results depending on the geographic location, community metrics and responses and spatio-temporal scales under study. For example, studies from the Beaufort Sea documented strong seasonal responses, such as increased SOD rates with increased ice algae standing stocks (Renaud et al., 2007) and a rise in benthic metabolic remineralization with an increase in food availability from spring to summer (Link et al., 2011). On the other hand, observations from the advective system of the European Arctic have supported the lack of pronounced seasonality in benthic community activities (Berge et al., 2015). Studies carried out in Kongsfjorden (West Spitsbergen) showed high resilience of macrofaunal food-web structure to seasonal variability in food quality (Kędra et al.2012) and unchanged size spectra of macro- and meiofauna between summer and winter (Mazurkiewicz et al. 2019). The seasonal stability in size spectra, food-web structure, abundance and biomass (Włodarska-Kowalczuk et al., 2016) and sediment oxygen demand (SOD) rates (Morata et al., 2020) of macrofaunal communities, in the same fjord, were attributed to the existence of a 'food bank' of detrital organic material stored year-round in sediments. The 'food bank' theory was first proposed as an explanation of the quasi-constant abundance patterns and the lack of seasonality in recruitment pulses in both macro- and megafauna and little seasonality in SOD rates observed on the shelf of the West Antarctic Peninsula (Smith et al., 2006; Glover et al., 2008). This apparent seasonal decoupling of benthic dynamics from pelagic processes had been only documented in Svalbard fjords. The fact that we observed so little seasonality in the taxonomic and functional composition of macrofauna community in our study could suggest that the northwestern Barents Sea shelf and adjacent basin present similar seafloor dynamics as that of the West Antarctic Peninsula shelf, which is also an advective system (Moffat & Meredith, 2018). This is supported by recent findings of moderate seasonality in SOD rates for the same study locations and seasons (Sen et al. unpublished data) and little variation in benthic food web structure (Ziegler et al., 2023). Thus, the 'food bank' theory could provide an explanation for analogous mechanism between advective polar environments of both hemispheres to sustain constant benthic communities year-round. Low bottom water temperatures in polar regions are hypothesized to be responsible for the relatively high preservation of food sources at the seafloor by hampering efficient bacterial remineralization (Smith et al., 2012 and references therein). Therefore, predicted increased bottom temperatures for the Barents Sea of up to 6 °C by the end of the 21st century (Renaud et al., 2019), could put the stability of this 'food bank' at risk (Smith et al., 2012 and references therein).

5. Conclusion

Our study revealed only weak signs of seasonality in macrofauna taxonomic composition and no seasonal variations in the analyzed metrics of functional composition in the northwestern Barents Sea. The constant total organic carbon in the sediments across seasons, in line with the non-seasonal community dynamics, might point towards the reliance of macrobenthos on the long-term accumulated food sources in the seafloor of this advective gateway, similarly as to what has been observed in other polar shelves such as the West Antarctic Peninsula.

Although no strong seasonal taxonomic variation was observed in macrofauna communities along the transect, functional composition remained much more constant across seasons. The relationship between functional diversity and taxonomic diversity for the whole transect, including all seasons, showed a significant, but not very strong linear relationship, indicating that the communities of the northwestern Barents Sea show a certain degree of functional resilience throughout all seasons (Kokarev et al., 2021). However, functional resilience was spatially heterogeneous, being much lower at the deep basin (P7 and SICE4) than communities on the shelf stations, most likely resulting from the very low taxonomic richness in these abyssal depths. This is in concordance with other studies showing that deep-sea macrofaunal assemblages from the eastern Fram Strait had lower functional redundancy than the shallower shelf (Górska et al., 2022). Therefore, the lack of seasonality that we observed in trait composition in our study might result from the relatively high functional resilience of the system, especially in the shelf, to slight fluctuations in species composition through time (seasons). This is consistent with the relatively constant benthic food-web structures found by Ziegler et al. (2023) for the same locations and across the same seasons.

It is anticipated that the timing of seasonal primary production will be affected by sea ice retreat and ocean warming driven by climate change. Therefore, fluctuations in the phenology of food export to the seafloor are to be expected. However, the year-round "food bank" on which macrobenthic communities may rely on, might buffer these shifts in the near future, making benthic communities resilient to changes in overlying waters. Nevertheless, regime shifts in productivity and abiotic drivers might cause integrated changes on longer time scales which might affect the stability of the sediment food bank, and thus, food availability. This could have implications for the ecological function and structure of macrobenthic communities in this region.

Funding

This study was financially supported by the Research Council of Norway (The Nansen Legacy, #276730). Internal funding was provided by Nord University, IOPAN (Project no 5226/Norway/2022/0 in the framework of Polish Ministry of Education and Science program PMW 2022-2023) and Akvaplan-niva.

CRediT authorship contribution statement

Èric Jordà-Molina: Investigation, Data curation, Formal analysis, Visualization, Writing – original draft, Writing – review & editing. **Arunima Sen:** Investigation, Data curation, Writing – review & editing, Supervision. **Bodil A. Bluhm:** Investigation, Data curation, Resources, Writing – review & editing, Supervision. **Paul E. Renaud:** Conceptualization, Resources, Writing – review & editing, Supervision. **Maria Włodarska-Kowalczuk:** Resources, Writing – review & editing. **Joanna Legeżyńska:** Investigation, Writing – review & editing. **Barbara Oleszczuk:** Investigation, Writing – review & editing. **Henning Reiss:** Supervision, Resources, Writing – review & editing.

Declaration of Competing Interest

The authors declare that they have no known competing financial interests or personal relationships that could have appeared to influence the work reported in this paper.

Data availability

Data will be made publicly available from 2024 on the Global Biodiversity Information Facility (GBIF) and will be accessible through the Svalbard Integrated Arctic Earth Observing System (SIOS).

Acknowledgements

We want to thank the crew from R/V *Kronprins Haakon* for all the support and logistics in the field. We also want to thank Thaise Ricardo de Freitas, Amanda Ziegler, Silvia Hess and Yasemin Bodur for their invaluable help collecting samples during the sampling campaigns. We thank Josquin Guerber and Antonia Mallmann for their help in sorting macrofauna samples in the lab. We also thank Martí Amargant Arumí for providing the script to assign the water masses definitions and Barbara Górska for advice on the FCA analysis. We thank all the logistics team from the Nansen Legacy project for their assistance during fieldwork.

Appendix A. Supplementary data

Supplementary data to this article can be found online at https://doi.org/10.1016/j.pocean.2023.103150.

References

Ahmed, D.A., van Bodegom, P.M., Tukker, A., 2019. Evaluation and selection of functional diversity metrics with recommendations for their use in life cycle assessments. Int. J. Life Cycle Assess. 24 (3), 485–500. https://doi.org/10.1007/s11367-018-1470-8.

Akvaplan-niva, 2023a. Nansen Legacy Sediment Pigment Data Q1 [Data set]. Norstore. https://doi.org/10.11582720203.00030.

Akvaplan-niva, 2023b. Nansen Legacy Sediment Pigment Data Q2 [Data set]. Norstore. https://doi.org/10.11582720203.00031.

Akvaplan-niva, 2023c. Nansen Legacy Sediment Pigment Data Q3[Data set]. Norstore. https://doi.org/10.11582720203.00032.

Akvaplan-niva, 2023d. Nansen Legacy Sediment Pigment Data Q4 [Data set]. Norstore. https://doi.org/10.11582720203.00033.

Ambrose Jr, W.G., Renaud, P.E., 1995. Benthic response to water column productivity patterns: Evidence for benthic-pelagic coupling in the Northeast Water Polynya. J. Geophys. Res. Oceans 100 (C3), 4411–4421. https://doi.org/10.1029/94JC01982.

Årthun, M., Ingvaldsen, R.B., Smedsrud, L.H., Schrum, C., 2011. Dense water formation and circulation in the Barents Sea. Deep Sea Res. Part I 58 (8), 801–817. https://doi.org/10.1016/j.dsr.2011.06.001.

Baird, D., Ulanowicz, R.E., 1989. The seasonal dynamics of the Chesapeake Bay ecosystem. Ecol. Monogr. 59 (4), 329–364. https://doi.org/10.2307/1943071.

Berge, J., Daase, M., Renaud, P.E., Ambrose, W.G., Darnis, G., Last, K.S., Leu, E., Cohen, J.H., Johnsen, G., Moline, M.A., 2015. Unexpected levels of biological activity during the polar night offer new perspectives on a warming Arctic. Curr. Biol. 25 (19), 2555–2561. https://doi.org/10.1016/j.cub.2015.08.024.

Beukema, J.J., 1974. Seasonal changes in the biomass of the macro-benthos of a tidal flat area in the Dutch Wadden Sea. Neth. J. Sea Res. 8 (1), 94–107. https://doi.org/10.1016/0077-7579(74)90028-3.

Bhaud, M.R., 1998. Species of Spiochaetopterus (polychaeta, Chaetopteridae) in the Atlantic-Mediterranean biogeographic area. Sarsia 83 (3), 243–263. https://doi.org/10.1080/00364827.1998.10413685.

Bivand, R.S., Pebesma, E.J., Gomez-Rubio, V., Pebesma, E.J., 2008. Applied Spatial Data Analysis with R, Vol. 747248717. Springer.

Blanchet, F.G., Legendre, P., Borcard, D., 2008. Forward selection of explanatory variables. Ecology 89 (9), 2623–2632. https://www.jstor.org/stable/27650800.

Bodur, Y.V., Renaud, P.E., Goraguer, L., Amargant-Arumí, M., Assmy, P., Dąbrowska, A. M., Reigstad, M., 2023. Seasonal patterns of vertical flux in the northwestern Barents Sea under Atlantic Water influence and sea-ice decline. Prog. Oceanogr., 103132 https://doi.org/10.1016/j.pocean.2023.103132.

Boon, A.R., Duineveld, G.C.A., 1996. Phytopigments and fatty acids as molecular markers for the quality of near-bottom particulate organic matter in the North Sea. J. Sea Res. 35 (4), 279–291. https://doi.org/10.1016/S1385-1101(96)90755-8.

Bourgeois, S., Archambault, P., Witte, U., 2017. Organic matter remineralization in marine sediments: A Pan-Arctic synthesis. Global Biogeochem. Cycles 31 (1), 190–213. https://doi.org/10.1002/2016GB005378.

Buettner, S., Ivanov, V. V, Kassens, H., Kusse-tiuz, N. A., Shipboard, T. H. E., & Team, S, 2020. Distribution of suspended particulate matter in the Barents Sea in late winter 2019. Arctic and Antarctic Research 66 (3), 267–278. https://doi.org/10.30758/0555-2648-2020-66-3-267-278.

Carmack, E., Wassmann, P., 2006. Food webs and physical–biological coupling on pan-Arctic shelves: unifying concepts and comprehensive perspectives. Prog. Oceanogr. 71 (2–4), 446–477. https://doi.org/10.1016/j.pocean.2006.10.004.

Carmona, C.P., De Bello, F., Mason, N.W.H., Lepš, J., 2016. Traits without borders: integrating functional diversity across scales. Trends Ecol. Evol. 31 (5), 382–394. https://doi.org/10.1016/j.tree.2016.02.003.

Carroll, J., Zaborska, A., Papucci, C., Schirone, A., Carroll, M.L., Pempkowiak, J., 2008. Accumulation of organic carbon in western Barents Sea sediments. Deep Sea Res. Part II 55 (20–21), 2361–2371. https://doi.org/10.1016/j.dsr2.2008.05.005.

Chevene, F., Doléadec, S., Chessel, D., 1994. A fuzzy coding approach for the analysis of long-term ecological data. Freshw. Biol. 31 (3), 295–309. https://doi.org/10.1111/j.1365-2427.1994.tb01742.x.

Cleary, A.C., Søreide, J.E., Freese, D., Niehoff, B., Gabrielsen, T.M., 2017. Feeding by Calanus glacialis in a high arctic fjord: potential seasonal importance of alternative prey. ICES J. Mar. Sci. 74 (7), 1937–1946. https://doi.org/10.1093/icesjms/fsx106.

Cochrane, S.K., Denisenko, S.G., Renaud, P.E., Emblow, C.S., Ambrose Jr, W.G., Ellingsen, I.H., Skarðhamar, J., 2009. Benthic macrofauna and productivity regimes in the Barents Sea—ecological implications in a changing Arctic. J. Sea Res. 61 (4), 222–233. https://doi.org/10.1016/j.seares.2009.01.003.

Cochrane, S.K.J., Pearson, T.H., Greenacre, M., Costelloe, J., Ellingsen, I.H., Dahle, S., Gulliksen, B., 2012. Benthic fauna and functional traits along a Polar Front transect in the Barents Sea-Advancing tools for ecosystem-scale assessments. J. Mar. Syst. 94, 204–217.

Coma, R., Ribes, M., Gili, J.M., Zabala, M., 2000. Seasonality in coastal benthic ecosystems. Trends Ecol. Evol. 15 (11), 448–453. https://doi.org/10.1016/S0169-5347(00)01970-4.

Daase, M., Falk-Petersen, S., Varpe, Ø., Darnis, G., Søreide, J.E., Wold, A., Leu, E., Berge, J., Philippe, B., Fortier, L., 2013. Timing of reproductive events in the marine copepod Calanus glacialis: a pan-Arctic perspective. Can. J. Fish. Aquat. Sci. 70 (6), 871–884. https://doi.org/10.1139/cjfas-2012-0401.

Degen, R., Aune, M., Bluhm, B.A., Cassidy, C., Kędra, M., Kraan, C., Vandepitte, L., Włodarska-Kowalczuk, M., Zhulay, I., Albano, P.G., 2018. Trait-based approaches in rapidly changing ecosystems: A roadmap to the future polar oceans. Ecol. Ind. 91, 722–736. https://doi.org/10.1016/j.ecolind.2018.04.050.

Degen, R., Faulwetter, S., 2019. The Arctic Traits Database – a repository of Arctic benthic invertebrate traits. Earth Syst. Sci. Data 11 (1), 301–322. https://doi.org/10.5194/essd-11-301-2019.

Descôteaux, R., Ershova, E., Wangensteen, O. S., Præbel, K., Renaud, P. E., Cottier, F., & Bluhm, B. A. (2021). Meroplankton Diversity, Seasonality and Life-History Traits Across the Barents Sea Polar Front Revealed by High-Throughput DNA Barcoding. In *Frontiers in Marine Science* (Vol. 8). https://doi.org/10.3389/fmars.2021.677732.

Dinno, A., Dinno, M.A., 2017. Package 'conover. test'. Conover-Iman Test of Multiple Comparisons Using Rank.

Dray, S., Blanchet, G., Borcard, D., Guenard, G., Jombart, T., Larocque, G., Legendre, P., Madi, N., Wagner, H.H., Dray, M.S., 2018. Package 'adespatial'. R Package 2018, 3–8.

Dray, S., Dufour, A.-B., 2007. The ade4 package: implementing the duality diagram for ecologists. J. Stat. Softw. 22, 1–20.

Dray, S., Pélissier, R., Couteron, P., Fortin, M.-J., Legendre, P., Peres-Neto, P.R., Bellier, E., Bivand, R., Blanchet, F.G., De Cáceres, M., Dufour, A.-B., Heegaard, E., Jombart, T., Munoz, F., Oksanen, J., Thioulouse, J., Wagner, H.H., 2012. Community ecology in the age of multivariate multiscale spatial analysis. Ecol. Monogr. 82 (3), 257–275. https://doi.org/10.1890/11-1183.1.

Dybwad, C., Lalande, C., Bodur, Y. V, Henley, S. F., Cottier, F., Ershova, E. A., Hobbs, L., Last, K. S., Dąbrowska, A. M., & Reigstad, M. (2022). The Influence of Sea Ice Cover and Atlantic Water Advection on Annual Particle Export North of Svalbard. *Journal of Geophysical Research: Oceans*, *127*(10), e2022JC018897. https://doi.org/https://doi.org/10.1029/2022JC018897.

Falk-Petersen, S., Pavlov, V., Berge, J., Cottier, F., Kovacs, K.M., Lydersen, C., 2015. At the rainbow's end: high productivity fueled by winter upwelling along an Arctic shelf. Polar Biol. 38 (1), 5–11. https://doi.org/10.1007/s00300-014-1482-1.

Fetzer, I., Arntz, W.E., 2008. Reproductive strategies of benthic invertebrates in the Kara Sea (Russian Arctic): adaptation of reproduction modes to cold water. Mar. Ecol. Prog. Ser. 356, 189–202. https://www.int-res.com/abstracts/meps/v356/p189-202/.

Gallucci, F., Moens, T., Fonseca, G., 2009. Small-scale spatial patterns of meiobenthos in the Arctic deep sea. Mar. Biodivers. 39, 9–25. https://doi.org/10.1007/s12526-009-0003-x.

Glover, A.G., Smith, C.R., Mincks, S.L., Sumida, P.Y.G., Thurber, A.R., 2008. Macrofaunal abundance and composition on the West Antarctic Peninsula continental shelf: Evidence for a sediment 'food bank' and similarities to deep-sea habitats. Deep Sea Res. Part II 55 (22), 2491–2501. https://doi.org/10.1016/j.dsr2.2008.06.008.

Górska, B., Gromisz, S., Legeżyńska, J., Soltwedel, T., Włodarska-Kowalczuk, M., 2022. Macrobenthic diversity response to the atlantification of the Arctic Ocean (Fram Strait, 79°N) – A taxonomic and functional trait approach. Ecol. Ind. 144, 109464 https://doi.org/10.1016/j.ecolind.2022.109464.

Graf, G., 1992. Benthic-pelagic coupling: a benthic view. Oceanogr. Mar. Biol. Annu. Rev.

Grebmeier, J.M., McRoy, C.P., Feder, H.M., 1988. Pelagic-benthic coupling on the shelf of the northern Bering and Chukchi seas. 1. Food supply source and benthic biomass. Marine Ecology Progress Series. Oldendorf 48 (1), 57–67. https://doi.org/10.3354/meps048057.

Hassel, A., 1986. Seasonal changes in zooplankton composition in the Barents Sea, with special attention to Calanus spp. (Copepoda). J. Plankton Res. 8 (2), 329–339. https://doi.org/10.1093/plankt/8.2.329.

Holm-Hansen, O., Lorenzen, C.J., Holmes, R.W., Strickland, J.D., 1965. Fluorometric determination of chlorophyll. ICES J. Mar. Sci. 30 (1), 3–15. https://doi.org/10.1093/icesjms/30.1.3.

Husum, K., Hald, M., Stein, R., Weißschnur, M., 2015. Recent benthic foraminifera in the Arctic Ocean and Kara Sea continental margin. Arktos 1, 1–17. https://doi.org/10.1007/s41063-015-0005-9.
Kędra, M., Kuliński, K., Walkusz, W., Legeżyńska, J., 2012. The shallow benthic food web structure in the high Arctic does not follow seasonal changes in the surrounding environment. Estuar. Coast. Shelf Sci. 114, 183–191. https://doi.org/10.1016/j.ecss.2012.08.015.
Klages, M., Boetius, A., Christensen, J.P., Deubel, H., Piepenburg, D., Schewe, I., Soltwedel, T., 2004. The benthos of Arctic seas and its role for the organic carbon cycle at the seafloor. The Organic Carbon Cycle in the Arctic Ocean 139–167. https://doi.org/10.1007/978-3-642-18912-8_6.
Kokarev, V.N., Vedenin, A.A., Basin, A.B., Azovsky, A.I., 2017. Taxonomic and functional patterns of macrobenthic communities on a high-Arctic shelf: a case study from the Laptev Sea. J. Sea Res. 129, 61–69. https://doi.org/10.1016/j.seares.2017.08.011.
Kokarev, V.N., Vedenin, A.A., Polukhin, A.A., Basin, A.B., 2021. Taxonomic and functional patterns of macrobenthic communities on a high Arctic shelf: A case study from the East Siberian Sea. J. Sea Res. 174, 102078. https://doi.org/10.1016/j.seares.2021.102078.
Kolde, R., 2019. pheatmap: Pretty Heatmaps. R-Project Org/Package= Pheatmap.
Kollsgård, C. T., Laberg, J. S., Rydningen, T. A., Forwick, M., Husum, K., and Lasabuda, A.: Sedimentary processes on the continental slope north of Kvitøya (northern Barents Sea) – preliminary results from regional bathymetry and sediment cores, EGU General Assembly 2021, online, 19–30 Apr 2021, EGU21-15494, https://doi.org/10.5194/egusphere-egu21-15494, 2021.
Laliberté, E., Legendre, P., Shipley, B., Laliberté, M., 2014. Measuring functional diversity from multiple traits, and other tools for functional ecology. R Package FD.
Lê, S., Josse, J., Husson, F., 2008. FactoMineR: an R package for multivariate analysis. J. Stat. Softw. 25, 1–18.
Legendre, P., Borcard, D., 2018. Box–Cox-chord transformations for community composition data prior to beta diversity analysis. Ecography 41 (11), 1820–1824. https://doi.org/10.1111/ecog.03498.
Legendre, P., De Cáceres, M., 2013. Beta diversity as the variance of community data: dissimilarity coefficients and partitioning. Ecol. Lett. 16 (8), 951–963. https://doi.org/10.1111/ele.12141.
Legendre, P., Gauthier, O., 2014. Statistical methods for temporal and space–time analysis of community composition data†. Proc. R. Soc. B Biol. Sci. 281 (1778), 20132728. https://doi.org/10.1098/rspb.2013.2728.
Leu, E., Mundy, C.J., Assmy, P., Campbell, K., Gabrielsen, T.M., Gosselin, M., Juul-Pedersen, T., Gradinger, R., 2015. Arctic spring awakening – Steering principles behind the phenology of vernal ice algal blooms. Prog. Oceanogr. 139, 151–170. https://doi.org/10.1016/j.pocean.2015.07.012.
Link, H., Archambault, P., Tamelander, T., Renaud, P.E., Piepenburg, D., 2011. Spring-to-summer changes and regional variability of benthic processes in the western Canadian Arctic. Polar Biol. 34 (12), 2025–2038. https://doi.org/10.1007/s00300-011-1046-6).
Lundesgaard, Ø., Sundfjord, A., Lind, S., Nilsen, F., Renner, A.H.H., 2022. Import of Atlantic Water and sea ice controls the ocean environment in the northern Barents Sea. Ocean Sci. 18 (5), 1389–1418. https://doi.org/10.5194/os-18-1389-2022.
Martinez Arbizu, P., 2017. PairwiseAdonis: pairwise multilevel comparison using Adonis. R Package.
Mazurkiewicz, M., Górska, B., Renaud, P.E., Legeżyńska, J., Berge, J., Włodarska-Kowalczuk, M., 2019. Seasonal constancy (summer vs. winter) of benthic size spectra in an Arctic fjord. Polar Biol. 42 (7), 1255–1270. https://doi.org/10.1007/s00300-019-02515-2.
Mincks, S.L., Smith, C.R., 2007. Recruitment patterns in Antarctic Peninsula shelf sediments: evidence of decoupling from seasonal phytodetritus pulses. Polar Biol. 30 (5), 587–600. https://doi.org/10.1007/s00300-006-0216-4.
Moffat, C., Meredith, M., 2018. Shelf–ocean exchange and hydrography west of the Antarctic Peninsula: a review. Philos. Trans. R. Soc. A Math. Phys. Eng. Sci. 376 (2122), 20170164. https://doi.org/10.1098/rsta.2017.0164.
Morata, N., Michaud, E., Włodarska-Kowalczuk, M., 2015. Impact of early food input on the Arctic benthos activities during the polar night. Polar Biol. 38, 99–114. https://doi.org/10.1007/s00300-013-1414-5.
Morata, N., Michaud, E., Poullaouec, M.-A., Devesa, J., Le Goff, M., Corvaisier, R., Renaud, P.E., 2020. Climate change and diminishing seasonality in Arctic benthic processes. Philos. Trans. R. Soc. A Math. Phys. Eng. Sci. 378 (2181), 20190369. https://doi.org/10.1098/rsta.2019.0369.
Morata, N., Renaud, P.E., 2008. Sedimentary pigments in the western Barents Sea: A reflection of pelagic–benthic coupling? Deep Sea Research Part II: Topical Studies in Oceanography 55 (20), 2381–2389. https://doi.org/10.1016/j.dsr2.2008.05.004.
Naumov, A.D., 2013. Long-term fluctuations of soft-bottom intertidal community structure affected by ice cover at two small sea bights in the Chupa Inlet (Kandalaksha Bay) of the White Sea. Hydrobiologia 706, 159–173. https://doi.org/10.1007/s10750-012-1339-y.
Oksanen, J., Blanchet, F.G., Kindt, R., Legendre, P., Minchin, P.R., O'hara, R. B., Simpson, G. L., Solymos, P., Stevens, M. H. H., & Wagner, H., 2013. Package 'vegan'. Community Ecology Package, Version 2 (9), 1–295.
Oug, E., Fleddum, A., Rygg, B., Olsgard, F., 2012. Biological traits analyses in the study of pollution gradients and ecological functioning of marine soft bottom species assemblages in a fjord ecosystem. J. Exp. Mar. Biol. Ecol. 432, 94–105. https://doi.org/10.1016/j.jembe.2012.07.019.
Pagès, J., 2004. Analyse factorielle de donnees mixtes: principe et exemple d'application. Revue De Statistique Appliquée 52 (4), 93–111.
Pawłowska, J., Włodarska-Kowalczuk, M., Zajączkowski, M., Nygård, H., Berge, J., 2011. Seasonal variability of meio-and macrobenthic standing stocks and diversity in an Arctic fjord (Adventfjorden, Spitsbergen). Polar Biol. 34, 833–845. https://doi.org/10.1007/s00300-010-0940-7.
Pebesma, E., Bivand, R.S., 2005. S classes and methods for spatial data: the sp package. R News 5 (2), 9–13.
Piepenburg, D., Ambrose Jr, W.G., Brandt, A., Renaud, P.E., Ahrens, M.J., Jensen, P., 1997. Benthic community patterns reflect water column processes in the Northeast Water polynya (Greenland). J. Mar. Syst. 10 (1–4), 467–482. https://doi.org/10.1016/S0924-7963(96)00050-4.
R Core Team, 2022. R: A language and environment for statistical computing. R Foundation for Statistical Computing, Vienna, Austria https://www.R-project.org/.
Reiss, H., Kröncke, I., 2005. Seasonal variability of infaunal community structures in three areas of the North Sea under different environmental conditions. Estuar. Coast. Shelf Sci. 65 (1–2), 253–274. https://doi.org/10.1016/j.ecss.2005.06.008.
Renaud, P.E., Riedel, A., Michel, C., Morata, N., Gosselin, M., Juul-Pedersen, T., Chiuchiolo, A., 2007. Seasonal variation in benthic community oxygen demand: A response to an ice algal bloom in the Beaufort Sea, Canadian Arctic? J. Mar. Syst. 67 (1), 1–12. https://doi.org/10.1016/j.jmarsys.2006.07.006.
Renaud, P.E., Morata, N., Carroll, M.L., Denisenko, S.G., Reigstad, M., 2008. Pelagic–benthic coupling in the western Barents Sea: Processes and time scales. Deep Sea Res. Part II 55 (20), 2372–2380. https://doi.org/10.1016/j.dsr2.2008.05.017.
Renaud, P.E., Ambrose, W.G., Węsławski, J.M., 2020. Benthic communities in the polar night. Polar Night Marine Ecology: Life and Light in the Dead of Night 161–179. https://doi.org/10.1007/978-3-030-33208-2.
Renaud, P.E., Wallhead, P., Kotta, J., Włodarska-Kowalczuk, M., Bellerby, R.G., Rätsep, M., Slagstad, D., Kukliński, P., 2019. Arctic sensitivity? Suitable habitat for benthic taxa is surprisingly robust to climate change. Front. Mar. Sci. 6, 538. https://doi.org/10.3389/fmars.2019.00538.
Rex, M.A., Etter, R.J., 2010. Deep-sea biodiversity: pattern and scale. Harvard University Press.
Ricardo de Freitas, T., Hess, S., Alve, E., Bluhm, B., Jordà Molina, È, Reiss, H., Renaud, P. E., Sen, A., Ziegler A. (2022a). Seabed sediment data (upper 6 cm) on water content, total nitrogen, total carbon, total organic carbon, total inorganic carbon, carbon and nitrogen isotopic composition from the Nansen Legacy seasonal cruise 2021703 (Q1). https://doi.org/10.21335/NMDC-1821375519.
Ricardo de Freitas, T., Hess, S., Alve, E., Bluhm, B., Jordà Molina, È, Reiss, H., Renaud, P. E., Sen, A., Ziegler A. (2022b). Seabed sediment data (upper 6 cm) on water content, total nitrogen, total carbon, total organic carbon, total inorganic carbon, carbon and nitrogen isotopic composition from the Nansen Legacy seasonal cruise 2021704 (Q2). https://doi.org/10.21335/NMDC-350572235.
Ricardo de Freitas, T., Hess, S., Alve, E., Bluhm, B., Jordà Molina, È, Reiss, H., Renaud, P. E., Sen, A., Ziegler A. (2022c). Seabed sediment data (upper 6 cm) on grain size, water content, total nitrogen, total carbon, total organic carbon, total inorganic carbon, carbon and nitrogen isotopic composition from the Nansen Legacy seasonal cruise 2019706 (Q3). https://doi.org/10.21335/NMDC-490057692.
Ricardo de Freitas, T., Hess, S., Alve, E., Bluhm, B., Jordà Molina, È, Reiss, H., Renaud, P. E., Sen, A., Ziegler A. (2022d). Seabed sediment data (upper 6 cm) on water content, total nitrogen, total carbon, total organic carbon, total inorganic carbon, carbon and nitrogen isotopic composition from the Nansen Legacy seasonal cruise 2019711 (Q4). https://doi.org/10.21335/NMDC-799257283.
Ricardo de Freitas, T. et al. 2023, this issue. Drivers of organic carbon distribution and accumulation in the northern Barents Sea. Progress in Oceanography (in review) (2023).
Rogge, A., Janout, M., Loginova, N., Trudnowska, E., Hörstmann, C., Wekerle, C., Oziel, L., Schourup-Kristensen, V., Ruiz-Castillo, E., Schulz, K., Povazhnyy, V.V., Iversen, M.H., Waite, A.M., 2023. Carbon dioxide sink in the Arctic Ocean from cross-shelf transport of dense Barents Sea water. Nat. Geosci. 16 (1), 82–88. https://doi.org/10.1038/s41561-022-01069-z.
Sakshaug, E., Johnsen, G.H., Kovacs, K.M., 2009. Ecosystem Barents Sea. Tapir Academic Press.
Saulnier, E., Brind'Amour, A., Tableau, A., Rufino, M.M., Dauvin, J.-C., Luczak, C., Le Bris, H., 2019. Seasonality in coastal macrobenthic biomass and its implications for estimating secondary production using empirical models. Limnol. Oceanogr. 64, 935–949. https://doi.org/10.1002/lno.11086.
Smith, C.R., DeMaster, D.J., Thomas, C., Sršen, P., Grange, L., Evrard, V., DeLeo, F., 2012. Pelagic-benthic coupling, food banks, and climate change on the West Antarctic Peninsula Shelf. Oceanography 25 (3), 188–201. http://www.jstor.org/stable/24861413.
Smith, C.R., Mincks, S., DeMaster, D.J., 2006. A synthesis of bentho-pelagic coupling on the Antarctic shelf: Food banks, ecosystem inertia and global climate change. Deep Sea Res. Part II 53 (8), 875–894. https://doi.org/10.1016/j.dsr2.2006.02.001.
Snelgrove, P.V.R., Soetaert, K., Solan, M., Thrush, S., Wei, C.-L., Danovaro, R., Fulweiler, R.W., Kitazato, H., Ingole, B., Norkko, A., 2018. Global carbon cycling on a heterogeneous seafloor. Trends Ecol. Evol. 33 (2), 96–105. https://doi.org/10.1016/j.tree.2017.11.004.
Solan, M., Bennett, E.M., Mumby, P.J., Leyland, J., Godbold, J.A., 2020. Benthic-based contributions to climate change mitigation and adaptation. Philos. Trans. R. Soc. B 375 (1794), 20190107. https://doi.org/10.1098/rstb.2019.0107.
Søreide, J.E., Carroll, M.L., Hop, H., Ambrose Jr, W.G., Hegseth, E.N., Falk-Petersen, S., 2013. Sympagic-pelagic-benthic coupling in Arctic and Atlantic waters around Svalbard revealed by stable isotopic and fatty acid tracers. Mar. Biol. Res. 9 (9), 831–850. https://doi.org/10.1080/17451000.2013.775457.
Steer, A. 2022. Nansen Legacy Stations – ice covered days. https://gitlab.com/adamsteer/aen/-/blob/main/jupyter-notebooks/ice-covered-days-only-sic.ipynb.
Sundfjord, A., Assmann, K.M., Lundesgaard, Ø., Renner, A.H.H., Lind, S., Ingvaldsen, R. B., 2020. Suggested water mass definitions for the central and northern Barents Sea,

and the adjacent Nansen Basin: Workshop Report. The Nansen Legacy Report Series 8. https://doi.org/10.7557/nlrs.5707.

Sutton, L., Mueter, F. J., Bluhm, B. A., & Iken, K. (2021). Environmental filtering Influences Functional Community Assembly of Epibenthic Communities . In *Frontiers in Marine Science* (Vol. 8). https://doi.org/10.3389/fmars.2021.736917.

Thamdrup, B., Canfield, D.E., 2000. Benthic respiration in aquatic sediments. Methods in Ecosystem Science 86–103. https://doi.org/10.1007/978-1-4612-1224-9_7.

Thorson, G., 1950. Reproductive and larval ecology of marine bottom invertebrates. Biol. Rev. 25 (1), 1–45. https://doi.org/10.1111/j.1469-185X.1950.tb00585.x.

van der Linden, P., Patrício, J., Marchini, A., Cid, N., Neto, J.M., Marques, J.C., 2012. A biological trait approach to assess the functional composition of subtidal benthic communities in an estuarine ecosystem. Ecol. Ind. 20, 121–133. https://doi.org/10.1016/j.ecolind.2012.02.004.

Vedenin, A., Budaeva, N., Mokievsky, V., Pantke, C., Soltwedel, T., Gebruk, A., 2016. Spatial distribution patterns in macrobenthos along a latitudinal transect at the deep-sea observatory HAUSGARTEN. Deep Sea Res. Part I 114, 90–98. https://doi.org/10.1016/j.dsr.2016.04.015.

Walsh, J.E., 2008. CLIMATE OF THE ARCTIC MARINE ENVIRONMENT. Ecol. Appl. 18 (sp2), S3–S22. https://doi.org/10.1890/06-0503.1.

Wassmann, P., Peinert, R., Smetacek, V., 1991. Patterns of production and sedimentation in the boreal and polar Northeast Atlantic. Polar Res. 10 (1), 209–228. https://doi.org/10.3402/polar.v10i1.6740.

Wassmann, P., Ratkova, T., Andreassen, I., Vernet, M., Pedersen, G., Rey, F., 1999. Spring Bloom Development in the Marginal Ice Zone and the Central Barents Sea. Mar. Ecol. 20 (3–4), 321–346. https://doi.org/10.1046/j.1439-0485.1999.2034081.x.

Wassmann, P., Carroll, J., Bellerby, R.G.J., 2008. Carbon flux and ecosystem feedback in the northern Barents Sea in an era of climate change: An introduction. Deep Sea Res. Part II 55 (20), 2143–2153. https://doi.org/10.1016/j.dsr2.2008.05.025.

Wassmann, P., Duarte, C.M., Agustí, S., Sejr, M.K., 2011. Footprints of climate change in the Arctic marine ecosystem. Glob. Chang. Biol. 17 (2), 1235–1249. https://doi.org/10.1111/j.1365-2486.2010.02311.x.

Wassmann, P., Carmack, E.C., Bluhm, B.A., Duarte, C.M., Berge, J., Brown, K., Grebmeier, J.M., Holding, J., Kosobokova, K., Kwok, R., 2020. Towards a unifying pan-arctic perspective: A conceptual modelling toolkit. Prog. Oceanogr. 189, 102455 https://doi.org/10.1016/j.pocean.2020.102455.

Wassmann, P., Reigstad, M., 2011. Future Arctic Ocean Seasonal Ice Zones and Implications for Pelagic-Benthic Coupling. Oceanography 24 (3), 220–231. http://www.jstor.org/stable/24861317.

Wassmann, P., Reigstad, M., Haug, T., Rudels, B., Carroll, M.L., Hop, H., Gabrielsen, G. W., Falk-Petersen, S., Denisenko, S.G., Arashkevich, E., Slagstad, D., Pavlova, O., 2006. Food webs and carbon flux in the Barents Sea. Prog. Oceanogr. 71 (2), 232–287. https://doi.org/10.1016/j.pocean.2006.10.003.

Weydmann, A., Søreide, J.E., Kwaśniewski, S., Leu, E., Falk-Petersen, S., Berge, J., 2013. Ice-related seasonality in zooplankton community composition in a high Arctic fjord. J. Plankton Res. 35 (4), 831–842. https://doi.org/10.1093/plankt/fbt031.

Włodarska-Kowalczuk, M., Górska, B., Deja, K., Morata, N., 2016. Do benthic meiofaunal and macrofaunal communities respond to seasonality in pelagial processes in an Arctic fjord (Kongsfjorden, Spitsbergen)? Polar Biol. 39 (11), 2115–2129. https://doi.org/10.1007/s00300-016-1982-2.

Włodarska-Kowalczuk, M., Aune, M., Michel, L.N., Zaborska, A., Legeżyńska, J., 2019. Is the trophic diversity of marine benthic consumers decoupled from taxonomic and functional trait diversity? Isotopic niches of Arctic communities. Limnol. Oceanogr. 64, 2140–2151. https://doi.org/10.1002/lno.11174.

Ziegler, A.F., Bluhm, B.A., Renaud, P.E., Jørgensen, L.L., 2023. Weak seasonality in benthic food web structure within an Arctic inflow shelf region. Prog. Oceanogr. 103109 https://doi.org/10.1016/j.pocean.2023.103109.

Zwarts, L., Wanink, J.H., 1993. How the food supply harvestable by waders in the Wadden Sea depends on the variation in energy density, body weight, biomass, burying depth and behaviour of tidal-flat invertebrates. Neth. J. Sea Res. 31 (4), 441–476. https://doi.org/10.1016/0077-7579(93)90059-2.